nagra National Cooperative for the Disposal of Radioactive Waste

TECHNICAL REPORT 95-06

A Quantitative Mechanistic Description of Ni, Zn and Ca Sorption on Na-Montmorillonite

Part III: Modelling

July 1995

M.H. Bradbury, B. Baeyens

PSI, Würenlingen and Villigen

Hardstrasse 73, CH-5430 Wettingen/Switzerland, Telephone +41-56-37 11 11

nagra National Cooperative for the Disposal of Radioactive Waste

TECHNICAL REPORT 95-06

A Quantitative Mechanistic Description of Ni, Zn and Ca Sorption on Na-Montmorillonite

Part III: Modelling

July 1995

M.H. Bradbury, B. Baeyens

PSI, Würenlingen and Villigen

Hardstrasse 73, CH-5430 Wettingen/Switzerland, Telephone +41-56-37 11 11

This report was prepared on behalf of Nagra. The viewpoints presented and conclusions reached are those of the author(s) and do not necessarily represent those of Nagra.

PREFACE

The Laboratory for Waste Management at the Paul Scherrer Institut is performing work to develop and test models as well as to acquire specific data relevant to performance assessments of Swiss nuclear waste repositories. These investigations are undertaken in close co-operation with, and with the financial support of, the National Cooperative for the Disposal of Radioactive Waste (Nagra). The present report is issued simultaneously as a PSI-Bericht and a Nagra Technical Report.

FOREWORD

This report is the third in a series of three, which together describe experimental investigations and modelling studies on the sorption of radionuclides by Na-montmorillonite. The aim of this work was to identify sorption mechanisms, develop mass action based models and determine the associated parameter values. In Part I the conditioning (purifying) procedures applied to the source material (SWy-1 Na-montmorillonite) are given together with characterisation and titration results. Sorption edge and isotherm data for Ni, Zn and Ca are presented in Part II. In a final report, Part III, an overall model was developed to describe the acid/base and sorption behaviour on Na-montmorillonite.

VORWORT

Der vorliegene Bericht ist der dritte aus einer Reihe von drei Berichten, die insgesamt die experimentellen Untersuchungen und Modellrechnungen zur Sorption von Radionukliden auf Na-Montmorillonit beschreiben. Ziel dieser Arbeit ist neben der Abklärung von Sorptionsmechanismen die Entwicklung von auf Massenwirkungsgesetzen basierenden Modellen und die Bestimmung der dazugehörigen Parameter. In Teil I werden Konditioniermethoden vorgestellt, mit Hilfe derer das Ausgangsmaterial (SWy-1 Na-Montmorillonit) aufgearbeitet wurde. Daneben werden Analysendaten und Ergebnisse der Titrationen vorgestellt. Teil II behandelt die pH-abhängige Sorption und Sorptionsisotherme von Ni, Zn und Ca. In Teil III wird abschliessend ein umfassendes Modell vorgestellt, welches neben dem Säure/Base-Verhalten der Oberflächengruppen auch die Sorptionseigenschaften von Na-Montmorillonit beschreibt.

PRÉFACE

Ce rapport est le troisième d'une série de trois rapports qui décrivent les travaux expérimentaux et le développement d'une modélisation concernant la sorption de radionucléides par la montmorillonite sodique conditionnée. Le travail présenté ici se focalise sur l'identification des mécanismes de sorption, le développement d'un modèle et la détermination des paramètres associés. Dans le premier rapport on décrit un procédé de conditionnement du matériel de base, la montmorillonite sodique (SWy-1), et, les données de caractérisation et de titration. Dans le deuxième rapport, les seuils de sorption et les isothermes de sorption qui ont été déterminés pour le Ni, le Zn et le Ca sont décrits. Dans le troisième rapport, un modèle est présenté qui reflète uniquement le comportement acide/base des sites de surface et la sorption sur la montmorillonite sodique conditionnée.

ABSTRACT

Titration and sorption measurements, carried out under a wide variety of conditions on Na-montmorillonite, were examined in terms of cation exchange and surface complexation mechanisms. A computer code called MINSORB was developed and used throughout this work. This code allowed the uptake of radionuclides by both mechanisms to be calculated simultaneously; also taking into account competitive reactions from other cations present. A stepwise iterative fitting/modelling procedure is described. For the case of Na-montmorillonite it is demonstrated that an electrostatic term in the surface complexation model is not required. A basic data set comprising of site capacities and protonation/deprotonation constants was defined, which was valid for all surface complexation sorption reactions. The main study was carried out with Ni, but impurity cations present in the system, particularly Zn, had to be examined in addition due to their competitive effects on Ni sorption. The surface complexation behaviour of Ni and Zn was investigated in detail to give intrinsic surface complexation constants on two of the $\equiv$SOH type sites included in the model. The sorption of Mg, Ca and Mn is also considered, though in less detail, and estimated surface complexation constants for these nuclides are presented. Cation exchange was included in all of the calculations. Measured selectivity coefficients for Ni-Na, Zn-Na and Ca-Na exchange reactions are given. The model, with the derived parameters, allowed all the data from titration measurements through sorption edges to sorption isotherms to be calculated.

ZUSAMMENFASSUNG

Titrations- und Sorptionsmessungen mit Na-Montmorillonit wurden unter verschiedenen Bedingungen durchgeführt und hinsichtlich Kationenaustausch und Oberflächenkomplexierungsmechanismen interpretiert. Zur Interpretation wurde ein Rechencode, MINSORB, entwickelt mit dem die Sorption der Radionuklide unter Berücksichtigung beider Mechanismen modelliert werden konnte. Der Code berücksichtigt zudem Konkurrenzreaktionen durch andere Kationen. Ein stufenweise iteratives Anpassungs-/Modellierungsverfahren wird beschrieben. Es wird gezeigt, dass zur Modellierung der Oberflächenkomplexierung kein elektrostatischer Term berücksichtigt werden muss. Ein grundlegender Datensatz für Na-Montmorillonit wurde bestimmt, der die Sorptionskapazitäten sowie Protonierungs-/Deprotonierungskonstanten enthält und für alle Oberflächenkomplexierungsreaktionen gültig war. Aus den detaillierten Untersuchungen zur Ni und Zn Sorption wurden intrinsische Komplexierungskonstanten für die zwei im Modell berücksichtigten ≡SOH-Oberflächengruppen bestimmt. Die Sorption von Mg, Ca und Mn wurde, obwohl weniger detailliert, ebenfalls untersucht, und Komplexierungskonstanten für diese Kationen konnten abgeleitet werden. In den Modellierungen wurden Kationaustauchprozesse mit den gemessenen Selektivitätskoefficienten Ni-Na, Zn-Na und Ca-Na jeweils mitberücksichtigt. Mit dem vorgestellten Modell können die experimentellen Daten der Titrationskurven, der pH-abhängigen Sorptionskurven wie auch der Sorptionsisothermen berechnet werden.

RÉSUMÉ

Des titrations et mesures de sorption effectuées sur de la montmorillonite sodique, sous des conditions variées, ont été examinées sous l'angle de l'échange cationique et des mécanismes de complexation de surface. Un programme informatique, le MINSORB, a été développé et utilisé pour ce travail. Ce programme permet de calculer simultanément la sorption de radionucléides par les deux mécanismes. Il prend en compte aussi les réactions concurrentes dues aux autres cations présents. On décrit la procédure de calibrage et de modélisation itérative par étapes. Pour le cas de la montmorillonite sodique, on montre qu'il n'est pas nécessaire d'inclure un terme électrostatique dans le modèle de complexation de surface. Un ensemble de données de base, comprenant des capacités des sites et des constantes pour la protonisation/déprotonisation, a été défini et reste valable pour toutes les réactions de sorption liées à la complexation de surface. L'étude principale a porté sur le Ni, mais d'autres cations, présents en tant qu'impuretés dans le système, en particulier le Zn, ont dû aussi être examinés en raison de leur effet concurrentiel sur la sorption du Ni. Le comportement de complexation de surface du Ni et du Zn a été étudié en détail, afin de définir les constantes intrinsèques de complexation de surface sur deux des sites du type ≡SOH contenus dans le modèle. La sorption du Mg, Ca et Mn a aussi été étudiée, quoique moins en détail, et une estimation des constantes de complexation de surface est fournie pour ces nucléides. L'échange cationique a été inclus dans tous les calculs. On fournit aussi les coefficients de sélectivité mesurés pour les réactions d'échange entre les couples Ni-Na, Zn-Na et Ca-Na. Le modèle, avec ses paramètres dérivés, permet de calculer toutes les données, des mesures de titration aux isothermes de sorption en passant par les seuils de sorption.

TABLE OF CONTENTS

LIST OF FIGURES

LIST OF TABLES

1 INTRODUCTION

This report describes the modelling work of the experimental titration and sorption data for conditioned Na-montmorillonite presented previously in Parts I and II respectively, (BAEYENS & BRADBURY, 1995a and b). The conditioning procedures applied to the source Na-montmorillonite (SWy-1, Crook County, Wyoming, USA), the physico-chemical characterisation results and titration curves for the purified Na-montmorillonite were given in Part I. Analyses of supernatant solutions from the batch titration tests formed an integral and important component of this work and the results showed that low levels of background impurity cations were present which could exert a significant influence on the form of titration curves and on sorption measurements. Consequently, although the bulk of the work described in Part II concerned the sorption behaviour of Ni on conditioned Na-montmorillonite, Zn and Ca were also investigated as important "impurity" cations present in the system. In order to provide a broad and diverse sorption data base for modelling, the uptake of Ni, Zn and Ca was measured in terms of sorption edges (log [distribution ratio] versus pH) and sorption isotherms over a wide range of conditions e.g. background electrolyte concentration, pH, solid to liquid (S:L) ratio and nuclide concentrations.

The three part format chosen for the presentation of this work was determined primarily by the philosophy behind the modelling methology, discussed in detail in Chapter 5. Briefly, fitting individual data sets in isolation often leads to ill-constrained and non-unique parameter sets. However, if a wide variety of data measured under a broad range of conditions is available, and the requirement is to model all the data with the minimum number of parameters, then the constraints on the model and the associated parameter values become severe. Hence, it was deemed necessary to describe all the experimental work first and to have all the various data sets available prior to beginning the modelling process. Data in the form of figures, tables and individual results will be taken from Parts I and II as required. For details of the experimental techniques and data analysis methods, the reader is referred to the original work.

2 SORPTION MECHANISMS

From the sorption measurements given in Chapters 9 to 11, three major trends in the data allow deductions to be made concerning likely sorption mechanisms. First, the sorption edge plots for Zn and Ni (see for example Figures 10 and 16) are typified by an initial constant distribution ratio region at low pH, followed by a strong increase in sorption as a function of pH. Secondly, the Ni sorption edge measurements carried out as a function of background electrolyte concentration, Figure 19, show clearly that at low pH the sorption varies strongly with the ionic strength whereas at high pH there is virtually no dependency. Finally, the general trend illustrated in the Ni isotherm plots in Figures 20 to 25 is that sorption tends to become more linear with decreasing pH and/or increasing nuclide concentration .

We have interpreted the above behaviour in terms of two different sorption mechanisms. The first mechanism tends to dominate the overall sorption under conditions of low pH and/or high sorbate concentrations. It is characterised by a pH independent linear sorption behaviour which is, however, very sensitive to the composition and major cation concentrations of the background electrolyte. As already described in Part II, Chapter 5, this mechanism, identified as cation exchange, was described in terms of selectivity coefficients defined according to GAINES & THOMAS (1953). The values of selectivity coefficients were calculated for Zn-Na, Ni-Na and Ca-Na from experimental sorption edge data measured at various $NaClO_4$ concentrations and are summarised in Table 1, section 4.2.

The second mechanism is characterised by a sorption behaviour which is strongly dependent on pH but essentially independent of the background electrolyte concentration. The contribution of this mechanism to the overall sorption will be discussed in terms of a surface complexation model (SC-model).

Sorption isotherms can sometimes be relatively complex, exhibiting a number of distinct regions of behaviour, see for example Figures 12 and 20. At low equilibrium concentrations the sorption is generally high and independent of concentration (Langmuir type). At intermediate concentrations the sorption is non-linear (Freundlich type), and at the highest concentrations the sorption

tends to become linear again. The extent to which each of these regions is present depends on the experimental conditions.

The broad picture which emerges from the isotherm data is that the linear sorption at the highest concentrations is attributed to cation exchange, whereas at intermediate and low equilibrium concentrations the results are compatible with a two site SC-model. The different site types associated with these two mechanisms are discussed further in Chapter 3.

Cation exchange and surface complexation mechanisms are operating simultaneously and hence the extent of nuclide uptake by one mechanism is influenced by sorption on the other. Which mechanism dominates depends on many factors such as pH, background electrolyte concentration and composition, cation exchange capacity, ≡SOH site capacities and equilibrium nuclide concentrations.

3 SORPTION SITE TYPES

The surfaces of Na-montmorillonite clay platelets carry a permanent negative charge arising from isomorphous substitution of lattice cations by cations of a lower valence e.g. divalent for trivalent cations in the octahedral layers and trivalent for tetravalent Si in the tetrahedral layers. Charge neutrality is maintained by the presence of an excess of cations in solution held electrostatically in close proximity around the outside of the Si-Al clay units. The electrostatically bound cations can undergo exchange with the cations in solution i.e. binding at these sites releases exchangeable cations of a stoichiometrically equivalent charge to maintain charge neutrality (GRIM 1953; NEWMAN 1987; VAN OLPHEN 1963; YARIV & CROSS 1979; BOLT & VAN RIEMSDIJK 1987).

The second category of sorption sites is perceived as being surface hydroxyl groups ($\equiv$SOH) situated along the edges of the clay platelets ("edge" or "broken bond" sites). Such sites can undergo protonation ($\equiv SOH_2^+$) or de-protonation ($\equiv SO^-$) reactions, and, because of this amphoteric behaviour, the uptake of nuclides varies strongly with pH. Depending on the surface complex formed, sorption releases one or more protons (GREENLAND & MOTT 1978; STUMM & MORGAN 1981; LAGALY & FAHN 1982; SPOSITO 1984).

In many systems sorption is observed to vary in a non-linear manner with the equilibrium concentration of the dissolved nuclide. For example, Freundlich sorption isotherms with gradients less than unity, and the shift of sorption edges to higher pH values as the sorbate to sorbent ratio increases (e.g. see DZOMBAK & MOREL 1990, Chapter 8), are typical and clear indicators that non-linear sorption processes are occurring.

It is relatively straightforward to appreciate that the minimum requirement for a description of non-linear sorption processes is either the sorption of a single species on two site types with different affinities or the sorption of two different species on one site type, again with different energies. When the surfaces of metal oxides are examined on an atomic scale there is spectroscopic evidence that there are a number of different surface hydroxyl groups present with varying acidities (SCHINDLER & STUMM 1987). Different crystal faces and imperfections such as steps and corners etc. can lead to sorption sites with

different energies. In reality there may be a whole spectrum of site types having different acid/base properties and sorption affinities. Interpretations based on site heterogeneity are generally more favoured in the open literature than multi species surface reactions (DAVIS & KENT 1990, DZOMBAK & MOREL 1990), though in some cases both are invoked (see for example WAITE et al. 1994).

Nevertheless, it should not be forgotten that models are developed to describe macroscopic observations and do not necessarily have to include all the detailed complexity of the microscopic processes. In most cases they represent simplifications, and not true reflections of reality. For example, it has been found in practice, at least for metal oxide systems, that a SC-model containing an electrostatic term and two site types is sufficient to reproduce a wide variety of sorption measurements in a reasonably satisfactory manner (DZOMBAK & MOREL 1990). The major criterion for judging the successfulness, or otherwise, of a model is its ability to predict sorption outside the range of conditions for which the model parameters were determined.

4 SORPTION MODELS

4.1 The Diffuse Double Layer Surface Complexation Model, DDL-Model

4.1.1 Model Description

In SC-models, sorption is described in terms of reactions between aqueous species and amphoteric ≡SOH type surface sites, generally with the release of one or more protons. Although various models have been proposed over the past 20 years or so to describe this process (see for example the review of DAVIS & KENT 1990), most were developed specifically for oxides and all are essentially based on the same fundamental concepts. Briefly, sorption is assumed to take place at specific surface sites having specific capacities and is described by mass action equations. The net surface charge is generally considered to be an important quantity and is determined by protonation and deprotonation reactions of the surface hydroxyl groups and by the sorbed species themselves. Mass action constants for surface reactions are modified by a correction factor which is a function of the surface charge and hence varies with pH and sorption.

In the absence of any compelling evidence in favour of selecting a more complex model, we have chosen to use the diffuse double layer model described by STUMM et al. (1970) and HUANG & STUMM (1973) because it is one of the simplest available and has fewer adjustable parameters than most comparable models. We will confine ourselves here to a brief description of the main model concepts and associated equations.

The oxide-water interface is described in terms of two layers of charge; a surface layer to which all specifically sorbed ions are assigned and a diffuse layer comprising of counter ions in solution (non-specifically sorbed ions). The distribution of ions in the diffuse layer is assumed to be described by the Gouy-Chapman equation. The relation between surface charge and potential is thus given by:

$$\sigma = 0.1174 \cdot C^{1/2} \cdot \sinh(Z\psi \cdot 19.46) \qquad [1]$$

where:

σ = surface charge density (coulombs m^{-2})

C = molar electrolyte concentration
Z = valence of electrolyte
ψ = surface potential (volts)

The surface hydroxyl groups (≡SOH) undergo protolysis reactions which generate a surface charge whose value varies with pH but has a maximum value equal to the number of binding sites.

$$\equiv SOH + H^+ \Leftrightarrow \equiv SOH_2^+ \quad [2]$$

and

$$\equiv SOH \Leftrightarrow \equiv SO^- + H^+ \quad [3]$$

where ≡SOH, $\equiv SOH_2^+$ and $\equiv SO^-$ are the neutral, positively and negatively charged surface hydroxyl groups.

A coulombic term, fixed by double layer theory, is used to model the continuous change in the apparent surface acidity constants as a function of pH. This coulombic or electrostatic term is written as:

$$\exp(\Delta Z \frac{F\psi}{RT}) \quad [4]$$

where:

ΔZ = is the change in charge of the surface species involved in a surface complexation reaction
F = Faraday constant (coulombs mol^{-1})
R = molar gas constant (coulombs mol^{-1} K^{-1})
T = absolute temperature (Kelvin)

The mass action equations corresponding to reactions [2] and [3], taking into account the electrostatic term, are given by:

$$K_{\text{int}}(+) = \frac{[\equiv SOH_2^+]}{[\equiv SOH]\cdot\{H^+\}} \exp(\frac{F\psi}{RT}) \quad [5]$$

$$K_{\text{int}}(-) = \frac{[\equiv SO^-]\cdot\{H^+\}}{[\equiv SOH]} \exp(-\frac{F\psi}{RT}) \quad [6]$$

where [ ] represents concentrations and { } activities. (The activity coefficients for surface species are assumed to be equal and surface activities are replaced by concentrations in the mass action equation). $K_{int}(+)$ and $K_{int}(-)$ are the intrinsic surface protonation and deprotonation constants respectively .

In an analogous manner, mass action equations can be written describing the surface complexation reaction of cationic species e.g. for a bivalent cation M^{2+}:

$$\equiv SOH + M^{2+} \Leftrightarrow \equiv SOM^{+} + H^{+} \qquad [7]$$

$$K_{int}(M) = \frac{[\equiv SOM^{+}]\cdot\{H^{+}\}}{[\equiv SOH]\cdot\{M^{2+}\}} \exp(\frac{F\psi}{RT}) \qquad [8]$$

$K_{int}(M)$ is the intrinsic surface complexation constant for M^{2+} in reaction [7].

As stated previously, SC-models were mainly developed for, and have been predominantly applied to, metal oxides. The nature and characteristics of the sorption sites on clay minerals such as Na-montmorillonite are probably somewhat different from those on metal oxides. Hence, though the basic concepts behind such SC-models may apply in general to clay minerals, they may not apply in detail. For the modelling exercise described in this work the DDL-model was taken as a starting point with the full realisation that some modifications might be necessary.

4.1.2 Summary of Parameters Required for the DDL-Model.

In the following we will list the model parameters required for a description of sorption based on a surface complexation (DDL-model) mechanism. We will indicate those parameters for which values can be measured (estimated) experimentally and those whose values are normally deduced from model fitting to experimental data. It should be recognised that fitting, or calibrating, exercises are intrinsic to the SC approach. As will be discussed in the next chapter, fitting/calibration should not be confused with predictive modelling.

Surface hydroxyl site capacity, ≡SOH
Although the magnitude of this term can be estimated from experiments,

the value obtained is often method dependent. (A critical review of the various methods can be found in JAMES & PARKS 1982.)
Estimates can be made using surface area measurements and a general site density value of 3.84 μmol m^{-2}, recommended for all minerals by DAVIS & KENT (1990).
In some cases the surface hydroxyl site capacity is obtained as a fit parameter and is fitted simultaneously with the surface acid/base constants to titration data (CHARLET et al. 1993; WANNER et al. 1994).
In the current work the total ≡SOH site capacity was obtained directly from the acid end-point of the titration curve for conditioned Na-montmorillonite, Part I, Chapter 7. This value of 8 x 10^{-2} mol of sites kg^{-1} was used as a non-adjustable parameter in all the calculations.

Strong site capacity, $\equiv S^{S}OH$
This is almost always a fit parameter having a value of a few % of the total site capacity.
However, good experimentally based estimates can be obtained from the appropriate sorption isotherm data. In Chapter 8 the procedure whereby an $\equiv S^{S}OH$ value of 2 x 10^{-3} mol kg^{-1} was obtained for conditioned Na-montmorillonite is described.

Weak site capacity, $\equiv S^{W}OH$
In a two site SC model the $\equiv S^{W}OH$ value is taken as being approximately equal to the total site capacity. The comments given above for the total ≡SOH site capacity are also valid here.

Surface acid/base constants.
The surface protonation, $K_{int}(+)$, and de-protonation, $K_{int}(-)$, constants are fit parameters obtained from titration data. Their magnitude depends on the value of the site capacity used in the SC-model.

Intrinsic SC constants for metal binding on strong and weak sites, $^{S}K_{int}(M)$ and $^{W}K_{int}(M)$.
$^{S}K_{int}(M)$ is a fit parameter obtained from sorption edge measurements. Its value is then fixed, and $^{W}K_{int}(M)$ is fitted to sorption isotherm data. The procedure for obtaining values for these two constants is illustrated in Chapters 9 and 11. Their magnitudes are again dependent on the strong and weak site capacities used in the model.

4.2 Cation Exchange and Summary of Parameters Required

The cation exchange model has already been fully described and discussed in Part II, Chapter 5, and only a summary of the main parameters is given here.

Cation exchange capacity, CEC
This is an experimentally determined parameter.
A value of $8.7 \pm 0.4 \times 10^{-1}$ eq kg^{-1} was measured for conditioned Na-montmorillonite using the ^{22}Na isotope dilution technique, Part I.

Selectivity coefficients, K_c
Experimentally determined parameters.
Selectivity coefficients for Zn, Ni and Ca with respect to Na were determined for conditioned Na-montmorillonite as a function of ionic strength at trace metal concentrations as described in Part II. The data are summarised below.

Table 1: Summary of calculated selectivity coefficients for the exchange of Ni-Na, Ca-Na and Zn-Na on Na-montmorillonite from experimentally measured sorption data.

Cation	$NaClO_4$ (M)	pH range	K_c (I=0)
Ni	0.1	<4.5	3.3
	0.03	<5.0	3.1
	0.01	<6.0	2.9
	0.003	<7.0	1.5
Ca	0.267	6.2	4.0
	0.1	<7.0	4.9
	0.03	<8.0	3.8
	0.001	<9.0	3.7
Zn	0.1	<3.0	3.9

It should be noted that selectivity coefficients are not thermodynamic constants and, depending on the system in question, their values may vary to a greater or lesser extent as a function of ionic strength and fractional cation occupancies on the exchanger; see for example the extensive review of BRUGGENWERT & KAMPHORST 1982).

5 MODELLING APPROACH

5.1 General

The terms "fitting" and "modelling" are often used interchangeably in the open literature. However, the two terms have distinctly different meanings and it is important to be clear what these differences are.

All of the parameters values required in SC-models cannot be measured independently, and hence fitting parameters to experimental data is an integral (initial) part of the modelling process. When an individual data set e.g. a titration curve or a sorption edge, is taken in isolation, it is generally an almost trivial exercise to find fit parameters which provide a good quantitative description of the measurements. Often, the parameter set is not unique, and others can be found which yield equally good fits. (See for example Chapter 7.) In such a situation it is almost impossible to make any judgement about the general validity of any of the sets of fitted parameters. However, if another, different set of measurements are available, and the fit parameters derived from the first data set become a fixed sub-set of parameters for a description of the second data set, then the overall constraints on the fit parameters increases. If several sets of measurements are available e.g. titration curves as a function of ionic strength, sorption data as a function of pH, ionic strength, nuclide inventories etc., and the aim is to find a self consistent data set with the minimum number of parameters describing all the available results, then the constraints on the parameters becomes very great indeed, and a fitting exercise develops into modelling work. If this stage can be reached, then the first step in testing the predictive capacity of the model is to apply it to data measured outside the range of conditions for which the model parameters were determined. Following this, predictions made for the sorption behaviour in complex water chemistries, for example, can be tested experimentally. The ability to correctly predict sorption over a wide variety of different conditions in a chosen system is the only relevant criteria for deciding upon the usefulness of a model. It is clear from the above that a significant quantity of measured data has to be in place before modelling can begin. (With too little data the constraints on the parameters are too weak and a fitting exercise results.)

We have tried to summarise the general approach adopted in the flow diagram given in Figure 1. It cannot be emphasised too strongly that the fitting procedure developed to determine the required parameters is an iterative exercise carried out over many data sets. Any parameter values fitted in one step are fixed for the subsequent steps. The process is continued until it is either successful or until it breaks down. A "break down" requires a return to some earlier step where a different approach or different fixed parameter sets or both are taken.

In the following section, and later in the more detailed descriptions of the titration and sorption calculations (Chapters 7 and 9 to 11), we have tried to illustrate how this iterative process works in practice. However, we should point out that the procedure is not quite as straightforward as indicated and only the main outlines have been given.

5.2 Procedure

Before starting the fitting procedure, it is clearly necessary to decide upon the conceptual models, sorption mechanisms and computer codes which are going to be used in the calculations. These selections must be seen as "initial choices" which can be modified or changed depending on the outcome of the fitting exercises.

Since the analysis of the titration data yield site capacities and acid/base constants required for all further calculations, the titration results are considered first. A successful conclusion to this stage in the procedure is attained when a parameter set is derived for the model which is capable of reproducing the titration curve, preferably at more than one background electrolyte concentration. Total site capacity, protonation, $K_{int}(+)$, and deprotonation, $K_{int}(-)$, constants are then fixed in the model for all subsequent sorption calculations.

Any consideration of sorption requires the surface complexation reaction to be defined. For the majority of sorbate-sorbent systems there is little or no independent information to guide the selection. Consequently, our initial choice was always the simplest ("chemically reasonable") surface complexation reaction, which, for a bivalent cation, is that given previously in equation 7.

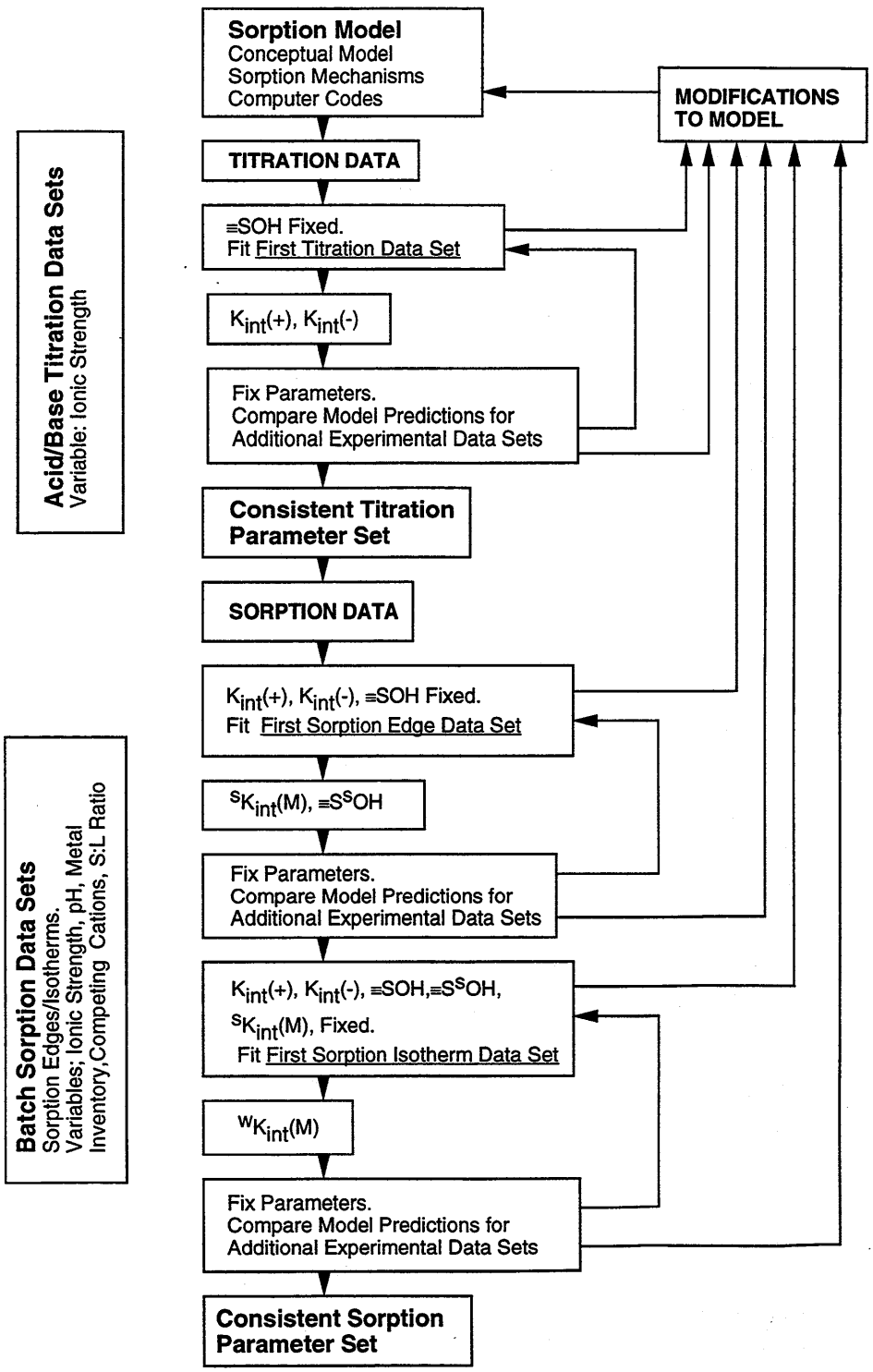

FIG. 1: Flow diagramme illustrating the iterative fitting/modelling procedure. (See section 4.1 for symbol definitions.)

In the specific case here, the isotherms measured for Zn and Ni, Figures 11 and 12, and 20 to 25 respectively, clearly exhibited a non-linear sorption dependency on the total aqueous equilibrium concentrations. In view of this, two site types were included in the SC-model, a small number of strongly sorbing sites ($\equiv S^{S}OH$) representing ~2.5% of the total, and weakly sorbing sites ($\equiv S^{W}OH$), see Chapters 3, 4 and 8. The form of the surface complex, and two sorption site types are choices for which there is at best only indirect supporting evidence.

Next, the sorption data for a specific nuclide are considered, starting with the sorption edge measurements. These measurements were always carried out at trace metal concentrations and S:L ratios which together ensured that sorption was only occurring on the strong sites. The parameters obtained from fits to such data, $\equiv S^{S}OH$ and ${}^{S}K_{int}(M)$, are not independent of one another. However, as will be shown in Chapter 8, independent estimates of the strong site capacity can be made from sorption isotherm data.

The weak site capacity is already fixed as the difference between the total site capacity and the strong site capacity and hence the only free parameter for fitting the SC-model to the sorption isotherm data is the complexation constant for the weak sites, ${}^{W}K_{int}(M)$. (The surface complex is assumed to be the same on both site types.)

Generally, an isotherm was chosen which exhibited the largest variation in the quantity sorbed over the widest concentration range. (For example, the Ni sorption isotherm given in Figure 20 is preferable to those in Figures 23 to 25.)

At this point all relevant parameters in the SC-model have been determined. These values are then fixed, and, as a first test of the model, predictions are made for the measured sorption data not used in the fitting procedure.

If this whole procedure can be completed successfully for one radionuclide, then the starting point for modelling the sorption of any other radionuclide is the same basic data set comprising of strong and weak site capacities and intrinsic acid/base constants. These are sorbent specific parameters which can no longer be changed i.e. they are fixed for all cations. The procedure is then the same as that outlined above.

6 MINSORB

In all of the fitting/modelling work described in the following chapters, a computer code called MINSORB was used. MINSORB is basically the geochemical speciation code MINEQL (WESTALL et al. 1976) containing a sub-routine for calculating sorption via the diffuse double layer surface complexation model. This model contains an electrostatic term in which the surface charge density is determined from the Gouy-Chapman relation. A further sub-routine allowed surface charge densities to be calculated for mixtures of asymmetric electrolytes (HUNTER 1981; DE LEVIE 1990). Activity corrections were carried out in the code using the Davies relation (DAVIES 1962). The thermodynamic data base compiled by PEARSON & BERNER (1991) and PEARSON et al. (1992) was used throughout.

In addition to surface complexation, sorption via the cation exchange mechanism was incorporated into the code (BRADBURY & BAEYENS 1994), and included in all the calculations given later using the selectivity coefficients listed in Table 1. (Cation exchange has already been discussed as a separate topic in Chapter 5, Part II, and is not treated further here.)

MINSORB is a relatively flexible code allowing speciation and sorption by cation exchange and surface complexation to be calculated simultaneously for any number of radionuclides in any given water chemistry on up to three different solid phases, each having up to ten different site types. Full sorption edges and isotherms can be calculated in a single run.

The general non-linear least squares optimisation programme FITEQL (WESTALL 1982) was available, but was not extensively used. Generally, FITEQL was applied to provide first estimates of parameter values from titration or sorption edge data. In practice we found the most efficient and satisfactory fitting procedure to be one of trial and error using MINSORB directly with experimentally measured and fixed parameter values together with first estimate values from FITEQL. Following the procedures outlined in the previous chapter implied that we were only fitting one parameter per data set in most cases.

7 TITRATIONS

7.1 Background

The experimentally determined net titration curves for conditioned Na-montmorillonite are given in Figure 2. The errors associated with the measurements, together with details of the data analysis, are fully discussed in Part I. The spread in the data points provide a reasonable indication of the uncertainty in the measured values. The errors are greater in the higher and lower pH regions as shown (i.e. pH >10.5; pH <3).

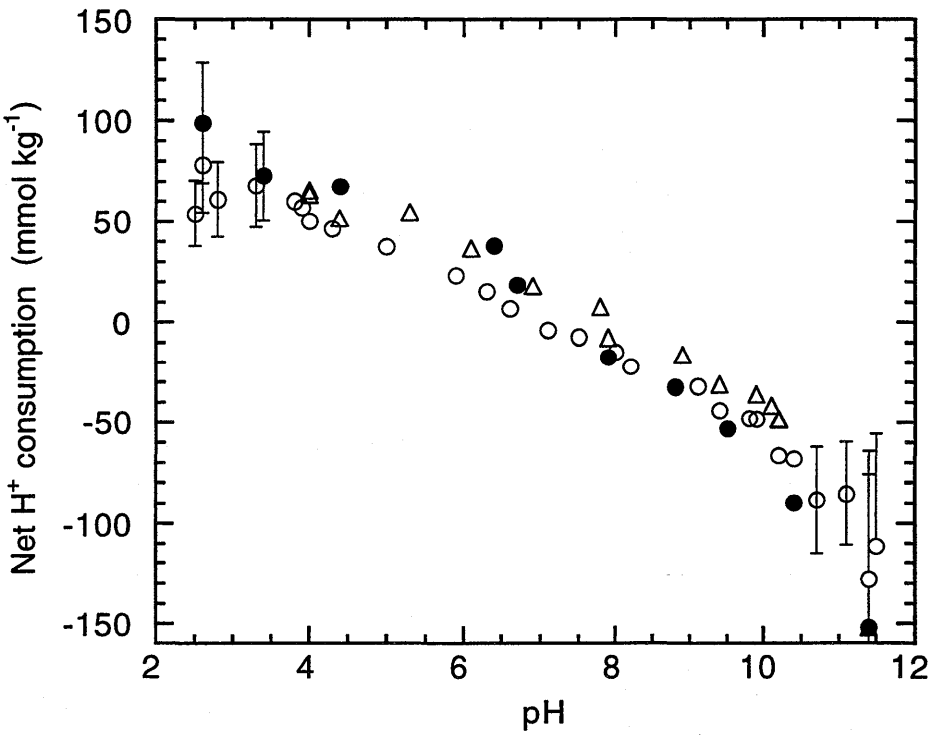

FIG . 2: Titration data for conditioned Na-montmorillonite:
0.5 M $NaClO_4$. Data measured after 1 day (O), and 7 days (●).
0.1 M $NaClO_4$. Data measured after 1 day (Δ).

The results indicate that neither ionic strength (0.1 and 0.5 M) nor kinetics (1 and 7 day experimental times) play a significant role in influencing the values of individual measurements, and consequently the overall form of the curve, over a wide pH range. The absence of any clear ionic strength dependency in the pH range investigated means that the titration data for Na-montmorillonite do not exhibit the cross-over point so typical for metal (hydr)oxide titration curves at different ionic strengths (e.g. see STUMM & MORGAN 1981). Results

reported for example by BEENE et al. (1991) on illites, and WANNER et al. (1994) on pre-treated MX-80 Bentonite, are in agreement with those presented here in that no clear intersections of the titration curves measured at different electrolyte concentrations were observed. Such behaviour is possibly a first indication that the standard DDL-model for oxides may not be appropriate for Na-montmorillonite, or, even more generally, for 2:1 type clay minerals.

The values of two important model parameters are already available from Part I.

(i) Multipoint N_2-BET measurements yielded a surface area value of 3.5×10^4 m^2 kg^{-1} for conditioned Na-montmorillonite. This value was fixed in all the following calculations.

(ii) From the end point in the acid region of the titration curve, a total $\equiv$SOH site capacity for conditioned Na-montmorillonite of 8×10^{-2} mol kg^{-1} was deduced; Part I, section 7.5. This value is a best estimate with an uncertainty in the region of ±25%.

The analysis of the titration data should yield intrinsic constants for the protonation, $K_{int}(+)$, and deprotonation, $K_{int}(-)$, reactions of the amphoteric $\equiv$SOH type surface sites. These constants, together with the site capacities, constitute the basic parameter set for Na-montmorillonite and are consequently critical to the modelling of sorption by this mechanism.

In the following we will describe in some detail the process by which $K_{int}(+)$ and $K_{int}(-)$ values were obtained in order to illustrate the points discussed and procedures given previously in Chapter 5.

7.2 DDL-Model

7.2.1 Titration Curve Calculations

We began the fitting process by applying the diffuse double layer model option in FITEQL to the 0.5 M $NaClO_4$ titration data using fixed values for the surface area and total site capacity of 3.5×10^4 m^2 kg^{-1} and 8×10^{-2} mol kg^{-1} respectively. The surface protolysis reactions and corresponding mass action equations are those given in section 4.1.1. The intrinsic protonation and deprotonation constants thereby obtained were then used in MINSORB to

produce a calculated titration curve which was compared with the experimental data. This was followed by an optimisation procedure in which the $K_{int}(+)$ and $K_{int}(-)$ values were systematically varied about their initial value to yield a best fit "by eye" to the titration curve, Figure 3(a).

All parameters were then fixed, and used to calculate a titration curve at 0.1 M $NaClO_4$, Figure 3(b). To some extent $K_{int}(+)$ and $K_{int}(-)$ can be optimised over both sets of data at this point, but the range of values over which this can be done is, in practice, relatively limited. The best fit curves are shown in Figure 3(c) together with all the experimental titration data. The parameter set used in the calculations is given in the figure caption.

Upon examination of Figure 3 it might be concluded that the fit achieved for the 0.5 M $NaClO_4$ data is good and, even if the correspondence between calculated and experimental data at 0.1 M $NaClO_4$ leaves something to be desired, the overall impression from Figure 3(c) is of a reasonable fit to the data. Although the DDL-model predicts a dependency on ionic strength with a "cross-over point", as would be expected since it was developed for oxides, this dependency is apparently relatively weak for Na-montmorillonite, and lies within the likely uncertainty band of the composite data sets. If only titration data were available, such a fit would be judged as being acceptable.

7.2.2 Test of DDL-Model Titration Parameters

Continuing the procedure proposed in Figure 1, the next step was to fix the model parameters used to fit the titration measurements and apply the model to sorption edge data. The Zn sorption edge results were chosen for this test.

As described in Chapter 3, the non-linear sorption characteristics of Zn on conditioned Na-montmorillonite imply that there are at least two sorbing site types involved in its uptake via a surface complexation mechanism. For the experimental conditions under which sorption edges were measured here, sorption is only occurring on the high affinity $\equiv S^{S}OH$ sites, see Chapter 5. These strong sites constitute only ~2.5% of the total $\equiv SOH$ site capacity and it is thus impossible to investigate their amphoteric behaviour separately. Therefore we follow the usual practice and make the assumption that their protolysis constants are the same as for the weak sites.

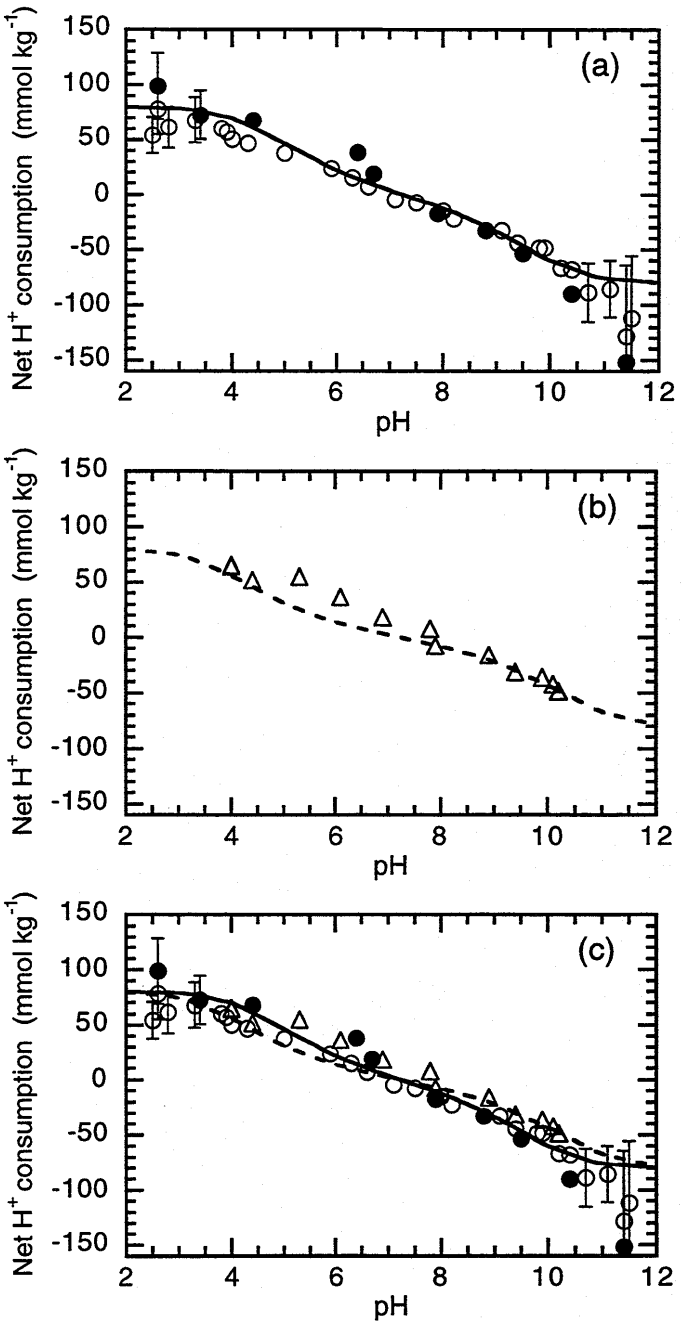

FIG. 3: Titration data for conditioned Na-montmorillonite.

(a) 0.5 M $NaClO_4$. Data measured after 1 day (O), and 7 days (●). The continuous line is a fit to the experimental data using the DDL-model.

Fixed parameters: Surface area: 3.5×10^4 m^2 kg^{-1};

Site capacity: 8×10^{-2} mol kg^{-1}.

Fitted parameters: log $K_{int}(+) = 6.2$; log $K_{int}(-) = -8.3$

(b) 0.1 M $NaClO_4$. Data measured after 1 day (Δ). The dashed line was calculated using the DDL-model and the parameters given above.

(c) Combined plot of experimental data and calculated titration curves.

For reactions of the form given in equation 7, there are normally two freely adjustable parameters available for fitting sorption edge data; the $\equiv S^SOH$ site capacity and the strong site surface complexation constant, $^SK_{int}(Zn)$. The combination of $\equiv S^SOH$ capacity and $^SK_{int}(Zn)$ determines the maximum value of sorption at any pH. Since their values are coupled, one parameter cannot be varied independently of the other. However, from the results and discussion given later in Chapter 8, an estimate for the strong site capacity was already available. Consequently, by fixing this value, FITEQL was only used to fit one parameter, $^SK_{int}(Zn)$, to the sorption edge. As with the titration calculations, MINSORB was then used and $^SK_{int}(Zn)$ varied to provide the best fit to the experimental data. Hence, when sorption edges are plotted as log R_d versus pH, and the $\equiv S^SOH$ capacity is fixed, the experimental data put tight restrictions on the range of values $^SK_{int}(Zn)$ may take. In addition, the position of the peak in a log R_d versus pH plot is essentially determined in the calculations by the $K_{int}(+)$, $K_{int}(-)$ and total site capacity parameters.* These are in turn fixed by the fits to the titration data. Two further characteristics of the measured sorption edges are important, namely, the slope of the rising edge of the curve and the ionic strength dependency. The chosen model together with the associated parameter set must also be able to reproduce these characteristics. Thus, it can be appreciated that even at this early stage in the fitting procedure, the scope for parameter variation is closing down rapidly.

In Figures 4(a) and (b) two attempts at fitting the experimental data are illustrated. Figure 4(a) represents the best fit achieved to the peak log R_d values, and Figure 4(b) the best fit obtained for the rising edge of the sorption curve. (It should not be forgotten that the only variable available for fitting these data was the $^SK_{int}(Zn)$ parameter.)

It is abundantly clear from Figure 4 that the fits are poor. The fundamental problem does not lie with the parameters values used to describe the sorption on the strong sites, since varying these only influences the peak maximum. Rather the peak position and the overall shape of the curve are incorrectly predicted.

---

* The formation of aqueous complexes can also potentially influence peak heights and position, see later in Chapter 12.

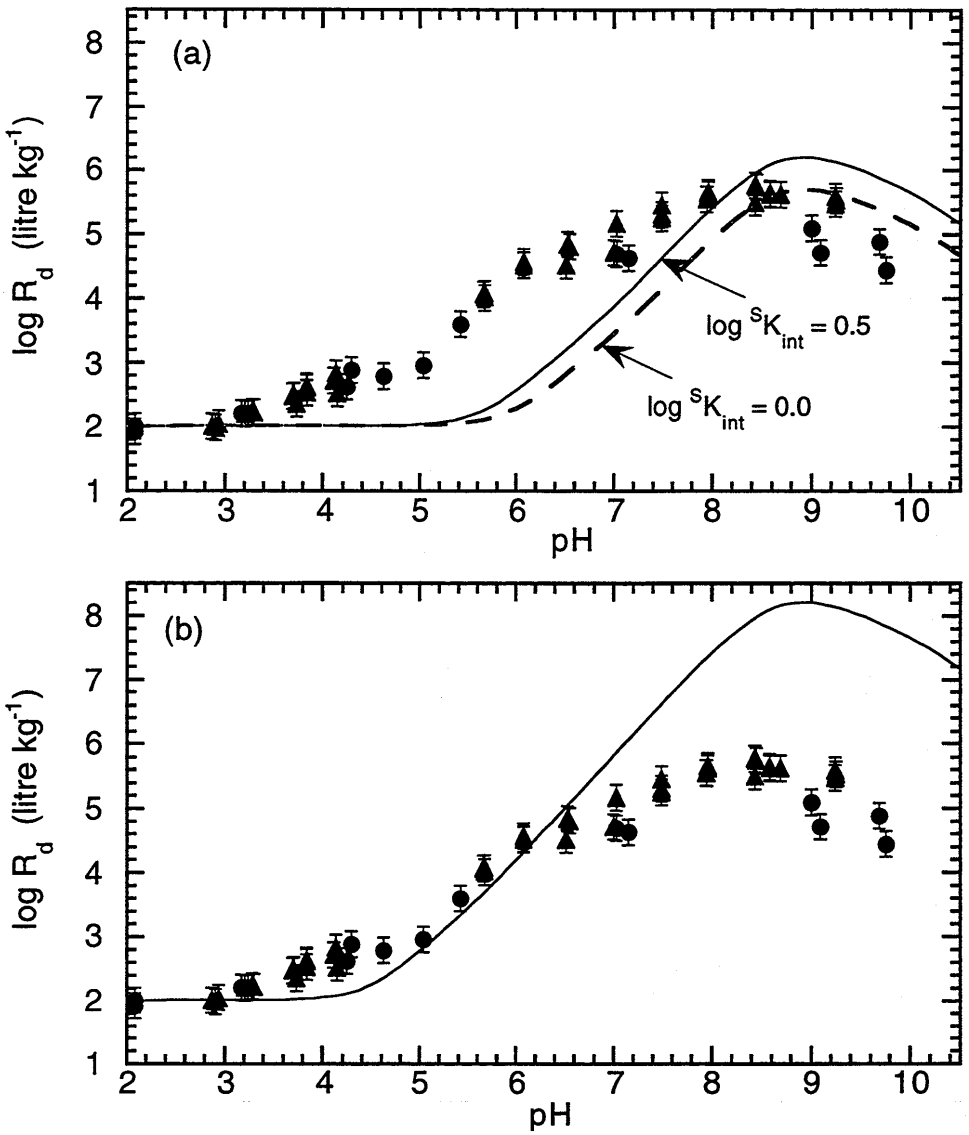

FIG. 4: Sorption edge data for Zn measured on Na-montmorillonite at 0.1 M $NaClO_4$.

(a) The lines are "best fits" obtained with the DDL-model to the peak log R_d values.

Fixed parameters: Zn inventory: 10^{-3} mol kg^{-1}; Surface area: 3.5×10^4 m^2 kg^{-1}; ≡SOH site capacity: 8×10^{-2} mol kg^{-1}; $\equiv S^{S}OH$ site capacity: 2×10^{-3} mol kg^{-1}; log $K_{int}(+) = 6.2$; log $K_{int}(-) = -8.3$;
CEC = 8.7×10^{-1} eq kg^{-1}; K_C (Zn-Na) = 3.9

Fitted parameter: log $^{S}K_{int}(Zn) = 0.5$ (continuous line);
log $^{S}K_{int}(Zn) = 0.0$ (broken line)

(b) The continuous line is the "best fit" obtained with the DDL-model to the rising edge of the sorption curve.

Fixed parameters: as given above.

Fitted parameter: log $^{S}K_{int}(Zn) = 2.5$

The curve shape can be changed, and the peak maximum broadened, but only by radically altering the values of $K_{int}(+)$, $K_{int}(-)$ and the site capacity. This, however leads to totally unacceptable fits to the titration data.

In addition, the rising edge for the experimental curve has a slope of ~1, whereas the gradient of the calculated curve is ~1.6. This is an important observation since the slope is a characteristic of the model and will not vary in any significant manner with the parameter data sets chosen.

Thus, we started from a position in which it appeared that the model was capable of satisfactorily reproducing titration data at two different ionic strengths. However, a subsequent application of the model to another, different set of data, in this case sorption edge measurements, revealed that the model was completely inadequate. The evidence available clearly indicates that modifications to the model are required in order to have any chance at all of being applicable to Na-montmorillonite. In terms of the flow diagramme given in Figure 1, we are now back at the starting point.

7.3 Model Modifications

At the end of the last section it was concluded that the DDL-model for oxides was not appropriate for describing the sorption characteristics of conditioned Na-montmorillonite. In particular, the slope of the rising edge of the log R_d versus pH plot was predicted to be ~1.6, rather than the experimentally measured value of ~1. The model exhibited serious short comings in other areas as well e.g. not being able to fit both rising edge position and peak height. However, the above was the key observation which indicated that the characteristics of the model predictions were at odds with experimental observation and, at the same time, indicated the direction in which the model should be modified. It is instructive to see, in a general way, how the dependency of log R_d on pH arises in the DDL-model.

In Chapter 5 we stated that in the absence of evidence to the contrary our choice of the SC reaction for a bivalent cation was governed mainly by simplicity and chemical reasonableness. Hence, a reaction of the form given in equation 7 was chosen. This reaction was expressed in a mass action relation by equation 8, which can in turn be re-expressed in the log form as:

$$\log R_d = \log K_{\text{int}}(M) - \log\{H^+\} - \log(\exp(\frac{F\psi}{RT})) + \log[\equiv SOH] + \log(\frac{L}{S}) + \log\frac{\{M^{2+}\}}{[M_{tot.}]} \quad [9]$$

where

$[M_{tot.}]$ = Total aqueous concentration of nuclide "M"
= $[M^{2+}]$ + [M-complexes]

$$R_d = \frac{[\equiv SOM^+]}{[M_{tot.}]} \cdot \frac{L}{S}$$

and

$\frac{L}{S}$ = liquid to solid ratio

In equation 9 two terms are constant, log K_{int}(M) and log(L/S) and in regions where the contribution of metal complexes to the total aqueous concentration of nuclide "M" is small, $\log\{M^{2+}\}/[M_{tot.}]$ can be neglected. Under these circumstances the factors determining the pH dependency of log R_d are log [≡SOH] and $-\log\{H^+\} - \log(\exp(F\psi/RT))$. The numerical values of log [≡SOH] and log $\exp(F\psi/RT)$ in the pH range from 4 to 10, appropriate for the sorption edges of Ni and Zn, are given in Table 2. From this table it is apparent that the variation of log [≡SOH] is relatively small, whereas the contribution from the electrostatic term increases by ~0.6 log units for each unit change in pH. The consequence is that log R_d is almost quadratically dependent on pH in the sorption edge plots.

If, on the other hand, the sorption edge occurs in a pH region where metal complexes readily form, then this will influence the slope of the rising edge via the $\log\{M^{2+}\}/[M_{tot.}]$ term in equation 9. The general effect of complexation, assuming only M^{2+} aqueous species form surface complexes, is to weaken the sorption dependency on pH.

In the DDL-model the relation between log R_d and pH is fixed by the surface complexation reaction, equation 7 i.e. the sorption of each Zn cation, for example, displaces a proton and increases the surface charge by +1 unit. We

were unable to devise a surface complexation reaction, even chemically unrealistic ones, which led to less than an exponent of ~1.6 for the dependency of log R_d on pH in the DDL-model. We concluded that the problem with the "fitting" did not lie with the choice of SC reaction or SC parameters, but rather with the model itself, and in particular the electrostatic term. The modification which readily suggested itself was to abandon "electrostatics" in the model.

Table 2: log [≡SOH] and the coulombic correction factor as a function of pH at 0.1 M $NaClO_4$. (Surface area = 3.5 x 10^4 m^2 kg^{-1}; Site capacity = 8 x 10^{-2} mol kg^{-1}, S:L = 1 gram $litre^{-1}$)

pH	log [≡SOH]	$-\log(\exp(F\psi / RT))$
4	-4.61	-1.85
5	-4.32	-1.38
6	-4.21	-0.80
7	-4.17	-0.16
8	-4.18	0.48
9	-4.25	1.10
10	-4.43	1.64

7.4 One Site Protolysis Model with No Electrostatic Term (1SPNE-Model)

7.4.1 Titration Curve Calculations

The procedure for using a single site protolysis model with no electrostatics to fit the titration data is much the same as that described in section 7.2.1, and only the main results will be given here. Basically, the same set of equations is used, but without the electrostatic term in the mass action relations.

Calculated titration curves for a fixed ≡SOH site capacity of 8 x 10^{-2} mol kg^{-1} are given in Figures 5 (a) to (c). The "best fit" achieved can only be described as reasonably acceptable since although the measured data are reproduced in a general sense, the correspondence between calculated and measured values on a more detailed level is not particularly good.

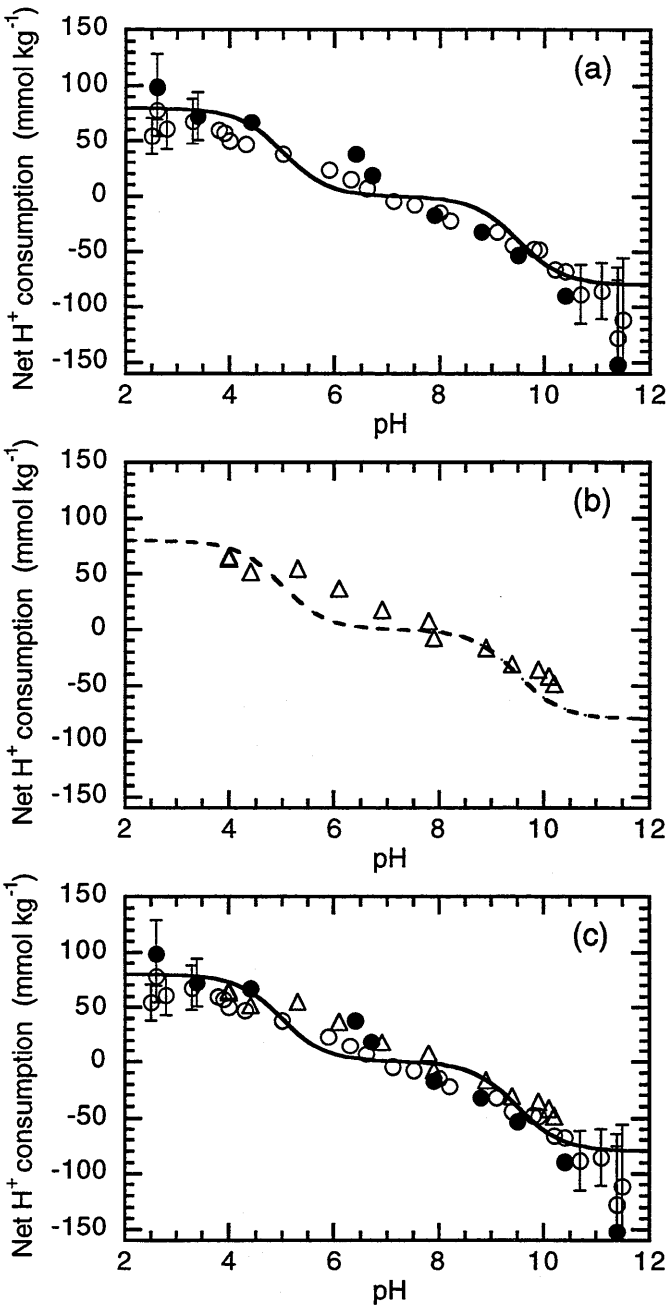

FIG. 5: Titration data for conditioned Na-montmorillonite.

(a) 0.5 M $NaClO_4$. Data measured after 1 day (O), and 7 days (●). The continuous line is a fit to the experimental data using the 1SPNE-Model.

Fixed parameters: Site capacity = 8×10^{-2} mol kg^{-1}.

Fitted parameters: log $K_{int}(+) = 5.0$; log $K_{int}(-) = -9.5$.

(b) 0.1 M $NaClO_4$. Data measured after 1 day (Δ). The dashed line was calculated using the 1SPNE-Model and the parameters given above.

(c) Combined plot of experimental data and calculated titration curves.

Nevertheless, it is worthwhile to continue to the next stage of the process and consider the Zn sorption edge data. It should be noted that the calculated curves for a non-electrostatic model show no dependency on ionic strength. Also, surface area is no longer a relevant parameter.

7.4.2 Test of Titration Parameters for the 1SPNE- Model

In a similar manner to that described in section 7.2.2, the Zn sorption edge measured at a $NaClO_4$ concentration of 0.1 M was fitted with the SC reaction given in equation 7 and the corresponding mass action relation without the electrostatic term. With fixed site densities and surface acid/base constants, best fits to the peak log R_d values and to the rising edge of the sorption curve are illustrated in Figures 6(a) and (b) respectively. The fit to the experimental data provided by the 1SPNE-model is considerably better than the DDL-model. The calculated slope of the rising edge is now correct but fitting the data with only one constant ($^{S}K_{int}(Zn)$) proved to be impossible. Either the position of the rising edge could be fitted, or the peak log R_d values, but not both. The overall curve shape again appears to be the main problem, and since acid/base constants play an important role in determining the form of sorption edges, and also because the fit to the titration data was not particularly good, the indications are that the titration data needs to be considered once more.

7.5 Two Site Protolysis Model with No Electrostatic Term (2SPNE - Model)

7.5.1 Titration Curve Calculations

Assuming that the basic model concepts are correct, the foregoing calculations indicated that the titration model was probably too simplistic and that there may be more than one ≡SOH site type involved in protonation/deprotonation reactions. A justification for introducing a second protolysis site type, still with an overall site capacity of 8×10^{-2} mol kg^{-1}, as the next logical step in increasing the complexity of the model, can be found in the structure of the edge surfaces created when phyllosilicate crystals are broken.

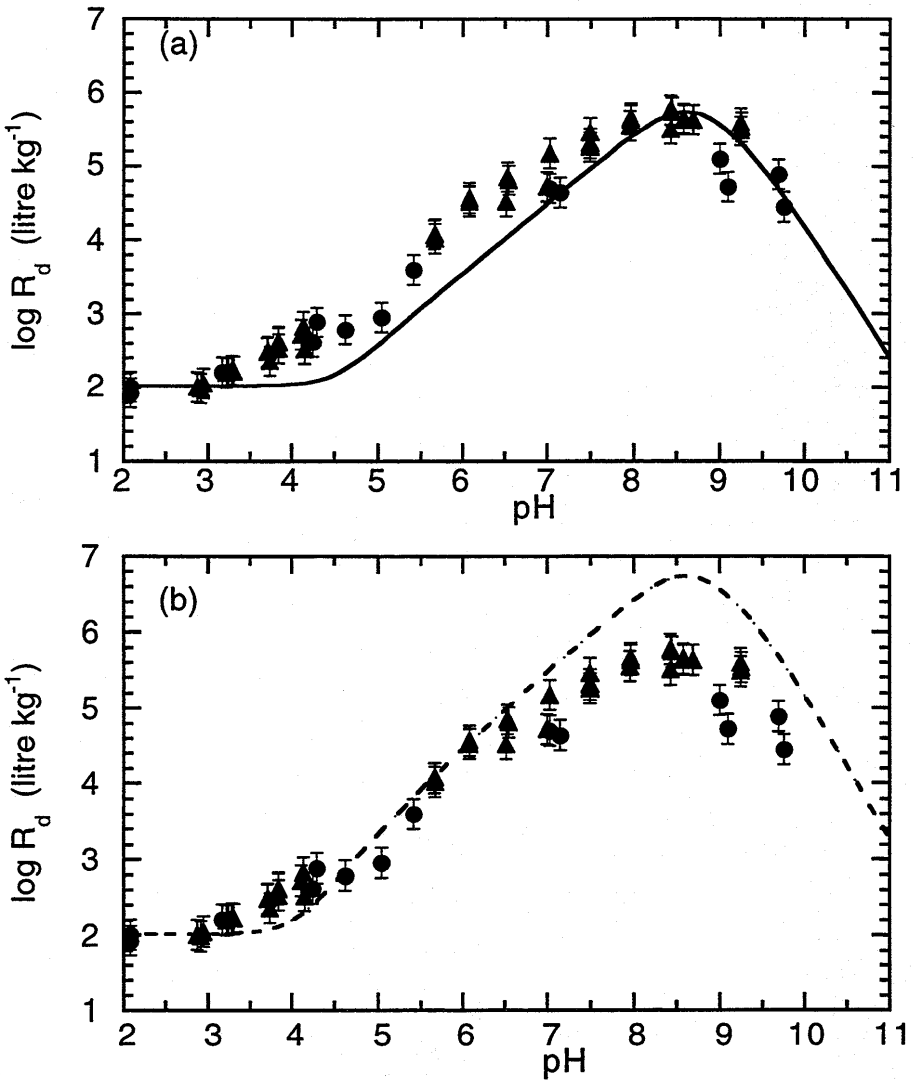

FIG. 6: Sorption edge data for Zn measured on Na-montmorillonite at 0.1 M $NaClO_4$.
(a) The continuous line is the "best fit" obtained with the 1SPNE-model to the peak log R_d values.
Fixed parameters: Zn inventory: 10^{-3} mol kg^{-1}
≡SOH site capacity: 8×10^{-2} mol kg^{-1}
≡S^SOH site capacity = 2×10^{-3} mol kg^{-1}
log $K_{int}(+) = 5.0$; log $K_{int}(-) = -9.5$
CEC = 8.7×10^{-1} eq kg^{-1}; K_c (Zn-Na) = 3.9
Fitted parameter: log $^SK_{int}(Zn) = 0.9$
(b) The dashed line is the "best fit" obtained with the 1SPNE-model to the rising edge of the sorption curve.
Fixed parameters: as given above
Fitted parameter: log $^SK_{int}(Zn) = 1.9$

SPOSITO (1984), BOLT & VAN RIEMSDIJK (1987) and FLETCHER & SPOSITO (1989) all present arguments to indicate that there are at least two distinct types of amphoteric surface hydroxyl functional groups; the so called silanol (≡SiOH) and aluminol (≡AlOH) sites.

Two protolysis site types means of course that the fit to the experimental titration data will be automatically improved, simply because there are now more adjustable parameters available. However, the aim is not just to find the best possible fit to the titration data by increasing the number of parameters, but rather to find the simplest model which is capable of describing the titration data adequately and also, with the acid/base constants fixed, a whole series of sorption data for different radionuclides at a variety of concentrations under different ionic strength and pH conditions. Thus, although the inclusion of a second protolysis site type would seem to justified by the observations made in the previous section, the appropriateness of such an increase in the complexity of the model will be checked further in subsequent sorption calculations.

Two protolysis site types imply that there are 6 unknown parameters: 2 site capacities and the four associated acid/base constants. The only boundary condition is that the sum of the two site capacities is fixed at 8×10^{-2} mol kg^{-1}. In a preliminary fitting phase the procedure adopted was to assume a ratio for the site capacities of 1:0.5 and then use FITEQL to provide an estimate of the 4 acid/base constants. This parameter set was then used in MINSORB to calculate the titration curve. This process was repeated for site ratios of 1:1, 1:1.5, etc. The outcome of this preliminary fitting exercise indicated an edge site ratio in the region of 1:1 to be the most appropriate. Using FITEQL and MINSORB to arrive at best fit values for the protolysis constants was considerably more time consuming than in previous similar exercises since the number of parameters involved was larger. The final calculated titration curves are shown in Figure 7. The capacities and acid/base constants for the 2 protolysis sites, $\equiv S^{W1}OH$ and $\equiv S^{W2}OH$, are given in the caption for Figure 7.

Unfortunately, we cannot claim that the combination of values given yields a unique best fit to the experimental titration data since an extensive systematic parameter variation exercise was not carried out. However, it is worth mentioning that the quality of the fits was very sensitive to the parameter values.

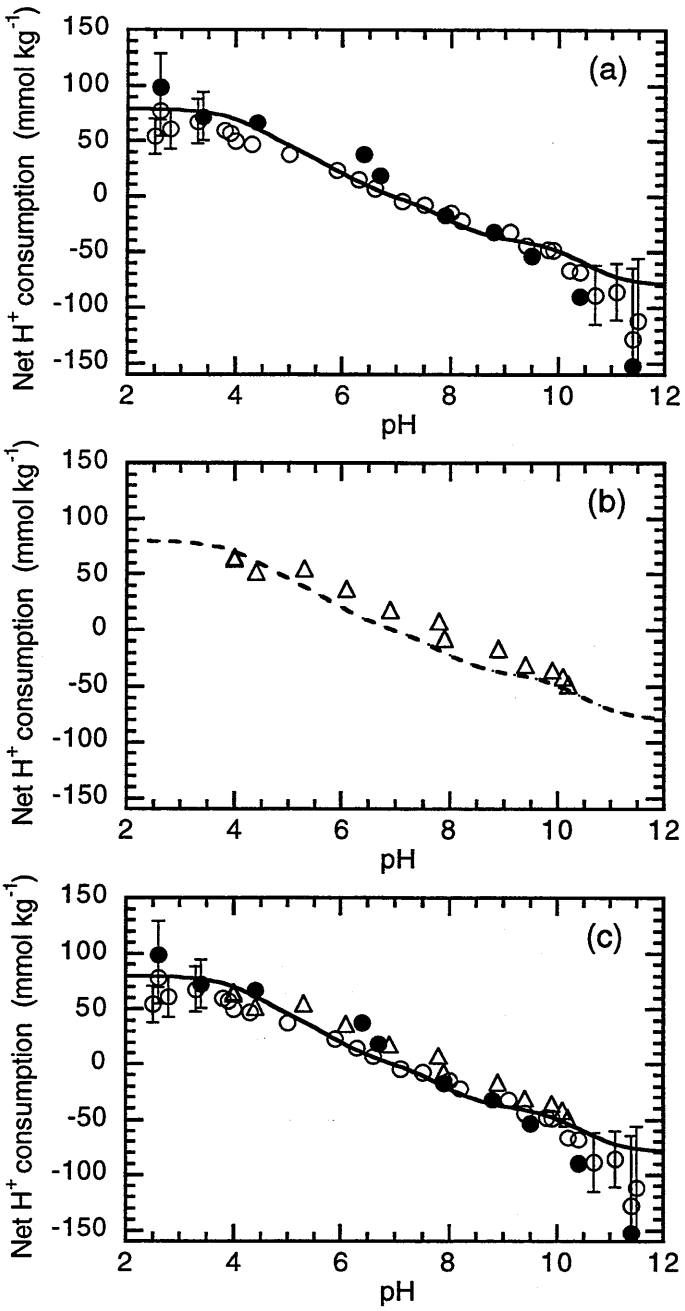

FIG. 7: Titration data for conditioned Na-montmorillonite.

(a) 0.5 M $NaClO_4$. Data measured after 1 day (O), and 7 days (●). The continuous line is a fit to the experimental data using the 2SPNE-Model.

Fixed parameters: Total site capacity = 8×10^{-2} mol kg^{-1}.

Fitted parameters: $\equiv S^{W1}OH$ site capacity: 4.0×10^{-2} mol kg^{-1}; log $K_{int}(+)$ = 4.5; log $K_{int}(-)$ = -7.9; $\equiv S^{W2}OH$: site capacity: 4.0×10^{-2} mol kg^{-1}; log $K_{int}(+)$ =6.0; log $K_{int}(-)$ = -10.5

(b) 0.1 M $NaClO_4$. Data measured after 1 day (Δ). The dashed line was calculated using the 2SPNE-Model and the parameters given above.

(c) Combined plot of experimental data and calculated titration curves.

7.5.2 Test of Titration Parameters for the 2 SPNE -Model

As in the other cases described, an initial fitting test was carried out on a Zn sorption edge measured at 0.1 M $NaClO_4$. As shown in Figure 8, the first application of the modified model with fixed site capacities and acid/base constants for the two weak site types, $\equiv S^{W1}OH$ and $\equiv S^{W2}OH$, can be fitted very well to the Zn sorption edge. Peak position, peak height, rising edge position and slope are all reproduced by the model using only the intrinsic SC constant for Zn on the strong sites as the variable parameter.

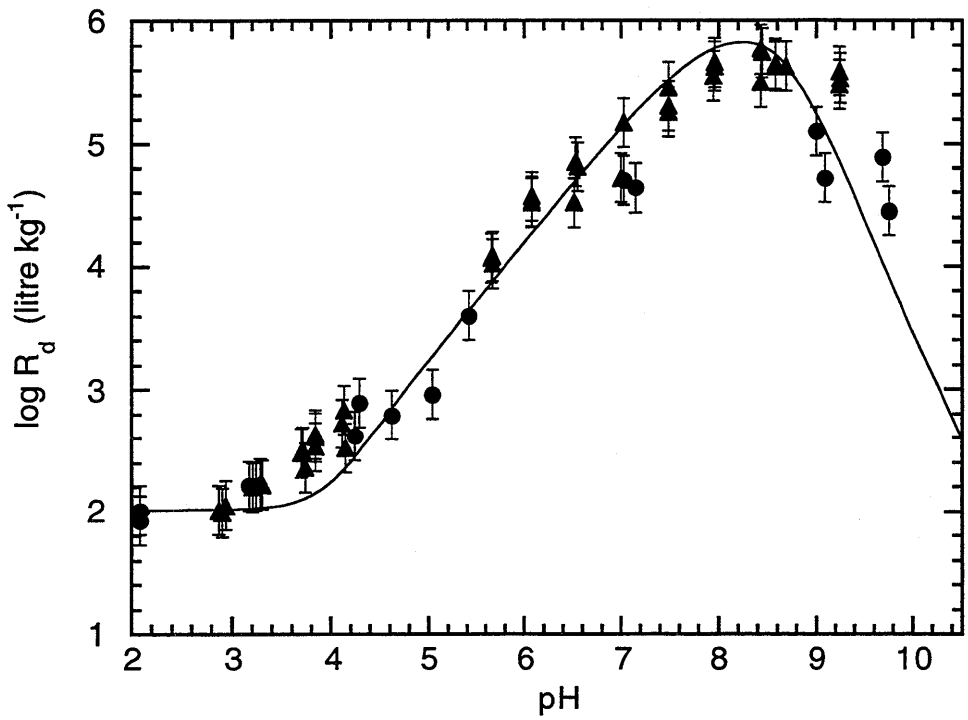

FIG. 8: Sorption edge data for Zn measured on Na-montmorillonite at 0.1 M $NaClO_4$. The continuous line is the "best fit" obtained with the 2SPNE-model.
Fixed parameters: Zn inventory: 10^{-3} mol kg^{-1}; Total site capacity: 8×10^{-2} mol kg^{-1}; $\equiv S^{S}OH$ site capacity: 2×10^{-3} mol kg^{-1}; $\equiv S^{W1}OH$ site capacity: 4.0×10^{-2} mol kg^{-1}; log $K_{int}(+)$ = 4.5; log $K_{int}(-)$ = -7.9; $\equiv S^{W2}OH$ site capacity: 4.0×10^{-2} mol kg^{-1}; log $K_{int}(+)$ = 6.0; log $K_{int}(-)$ = -10.50 ; CEC: 8.7×10^{-1} eq kg^{-1} ; K_c(Zn-Na) = 3.9
Fitted parameter: log $^{S}K_{int}(Zn)$ = 1.6

The main findings of this chapter regarding the titration calculations are two-fold. First, for the chosen approach and model, the accumulated evidence points strongly to the fact that an electrostatic term is not required. Indeed, the inclusion of such a term predicts entirely the wrong characteristics for the measured Zn sorption edge. Secondly, two protolysis site types appear to be necessary to provide an adequate description of the titration data and sorption edge measurements. The protonation/deprotonation constants and site capacities play a central role in determining the position and form of the sorption edge. At this stage a parameter data set describing the amphoteric behaviour of ≡SOH type sites on Na-montmorillonite in a non-electrostatic SC-model can be fixed. The parameter values so far determined are summarised in Table 3 and become non-adjustable quantities in all the following calculations.

Table 3: Summary of site types, site capacities, protolysis reactions and constants for conditioned Na-montmorillonite

Site type:	Site capacity:
Strong: $\equiv S^{S}OH$	2.0×10^{-3} moles kg^{-1}
Weak 1: $\equiv S^{W1}OH$	4.0×10^{-2} moles kg^{-1}
Weak 2: $\equiv S^{W2}OH$	4.0×10^{-2} moles kg^{-1}

Surface complexation reaction	Mass action equation	log K_{int}
$\equiv S^{S}OH + H^{+} \Leftrightarrow \equiv S^{S}OH_2^{+}$	$K_{int}(+) = \frac{[\equiv S^{S}OH_2^{+}]}{[\equiv S^{S}OH]\cdot\{H^{+}\}}$	4.5
$\equiv S^{S}OH \Leftrightarrow \equiv S^{S}O^{-} + H^{+}$	$K_{int}(-) = \frac{[\equiv S^{S}O^{-}]\cdot\{H^{+}\}}{[\equiv S^{S}OH]}$	-7.9
$\equiv S^{W1}OH + H^{+} \Leftrightarrow \equiv S^{W1}OH_2^{+}$	$K_{int}(+) = \frac{[\equiv S^{W1}OH_2^{+}]}{[\equiv S^{W1}OH]\cdot\{H^{+}\}}$	4.5
$\equiv S^{W1}OH \Leftrightarrow \equiv S^{W1}O^{-} + H^{+}$	$K_{int}(-) = \frac{[\equiv S^{W1}O^{-}]\cdot\{H^{+}\}}{[\equiv S^{W1}OH]}$	-7.9
$\equiv S^{W2}OH + H^{+} \Leftrightarrow \equiv S^{W2}OH_2^{+}$	$K_{int}(+) = \frac{[\equiv S^{W2}OH_2^{+}]}{[\equiv S^{W2}OH]\cdot\{H^{+}\}}$	6.0
$\equiv S^{W2}OH \Leftrightarrow \equiv S^{W2}O^{-} + H^{+}$	$K_{int}(-) = \frac{[\equiv S^{W2}O^{-}]\cdot\{H^{+}\}}{[\equiv S^{W2}OH]}$	-10.5

8 DETERMINATION OF THE STRONG SITE CAPACITY, $\equiv S^SOH$, FOR CONDITIONED Na-MONTMORILLONITE

The two model parameters required to calculate sorption edges are the $\equiv S^SOH$ site capacity and the surface complexation constant, ${}^SK_{int}(M)$. Both are almost always fit parameters. Although in principle strong site capacities can be obtained experimentally, direct measurements are difficult and uncertain, with estimates often varying over an order of magnitude or more, see for example section 4.3 in DZOMBAK & MOREL (1990). In this work we were able to determine a value for the strong site capacity and the procedure is outlined below.

If we consider the Ni sorption isotherm plot for pH=8.2, reproduced in Figure 9, it can be readily appreciated that there are two distinct regions. At higher concentrations (broken line) the curve has a slope of ~ 0.6 which is indicative of non-linear sorption. At lower concentrations the slope tends to unity (dotted line), representing a linear sorption behaviour. For the model concepts used here, this linear region (Langmuir type sorption) represents the uptake of Ni by a single site type i.e. sorption on the strong $\equiv S^SOH$ type sites. The intersection of the two lines in Figure 9 represents the change-over point between linear and non-linear sorption or in other words the approximate point at which the strong sites become saturated. The quantity of Ni on the solid at this point is ~ 3×10^{-4} mol kg^{-1}, and for a surface species of the form $\equiv S^SONi^+$, is directly equivalent to the number of surface sites occupied.

If no further information were to be available, then 3×10^{-4} mol kg^{-1} would probably have been the best estimate for the strong site capacity. However, additional data are available from the characterisation studies for conditioned Na-montmorillonite reported in Part I. We know from these measurements that there is a Zn inventory of ~ 10^{-3} mol kg^{-1}. Also we know that Zn sorbs considerably more strongly than Ni, see Chapter 9. Assuming that they are both sorbing on the same strong sites, then the Ni occupancy calculated above is in addition to the Zn already sorbed as $\equiv S^SOZn^+$ i.e. the total quantity of Zn plus Ni sorbed is ~ 1.3×10^{-3} mol kg^{-1}. In addition, we know from Part I that Mn is also present in the conditioned Na-montmorillonite system with an inventory of ~ 4×10^{-4} mol kg^{-1} and that the sorption characteristics of Mn are somewhat similar to Ni (see Chapter 10).

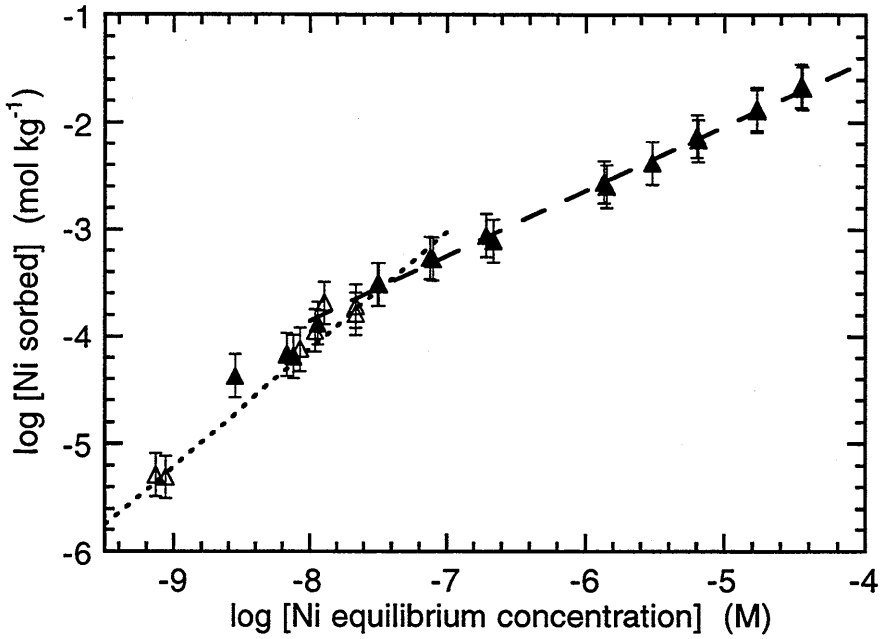

FIG. 9: Ni sorption isotherm data on conditioned Na-montmorillonite at pH = 8.2 and at 0.1 M $NaClO_4$. (Data are taken from Figure 16, Part II.)
Broken line: Freundlich type sorption (Gradient = 0.6± 0.01)
Dotted line: Langmuir type sorption (Gradient = 1.1± 0.1).

Consequently, most of this Mn, as in the case for Zn, is already sorbed onto the strong sites at pH > 8, yielding a new estimate of the strong site capacity of ~ 1.7×10^{-3} mol kg^{-1}. The error in this estimate could easily be ±50% because of the uncertainties in the absolute values for the Zn and Mn inventories and because site saturation by Ni at pH = 8.2 may not have been complete. Taking all the available information into account, a value of 2×10^{-3} mol kg^{-1} was selected for the strong site capacity. The magnitude of this parameter is now fixed and used throughout all the following calculations.

The above illustrates that values for the strong site capacities estimated only from isotherm measurements can be significantly in error. The influence of background impurities in the system must be considered. These impurities can arise either from the solid phase itself or may be added inadvertently with the "impure" electrolyte solutions. The influence of impurities on estimates of the strong site capacities may be, at least in part, an explanation for the discrepancies in these values found depending on the sorbing cation and/or the S:L ratio used in the sorption experiments (see again section 4.3 in DZOMBAK & MOREL 1990).

9 ZINC SORPTION

9.1 General

Using the titration parameter set given in Table 3 as fixed values, we now turn to the edge and isotherm sorption measurements. We noted in Part I that Zn was a ubiquitous impurity present in the conditioned Na-montmorillonite system at a level of ~ 10^{-3} mol kg^{-1}. Since Zn may influence the sorption behaviour of other radionuclides by competing with them for the available sorption sites, particularly at trace concentration levels, its sorption behaviour was investigated separately. Sorption edge measurements gave a clear indication that at low concentrations the affinity of Zn for the strong $\equiv S^SOH$ type sites was considerably greater than Ni, the principle nuclide being investigated. (Compare for example the sorption edges for Zn and Ni in Figures 10 and 16. It can clearly be seen that the Zn edge begins to rise strongly at a pH value approximately one unit lower than Ni.) Hence, in order to be able to model the sorption of Ni, the sorption behaviour of Zn had to be quantified and for this reason the Zn data are considered here first.

9.2 Zinc Sorption Edges

Since in the previous chapter we have fixed the value of the $\equiv S^SOH$ site capacity, the only adjustable parameter available for fitting the sorption edge is the surface complexation constant, ${}^SK_{int}(Zn)$, for a reaction of the form given in equation 7. The fitting procedures for the sorption measurements are similar in principle to those previously described for the titration data i.e. FITEQL is used to provide a first estimate of ${}^SK_{int}(Zn)$ and then variations about this value are used in MINSORB to give the "best fit" over the whole sorption edge.

The best fit found for the Zn sorption edge data is shown in Figure 10 by the continuous line. In the model calculations the decrease in sorption at pH values greater than approximately 8.5 is due to aqueous phase hydrolysis reactions.

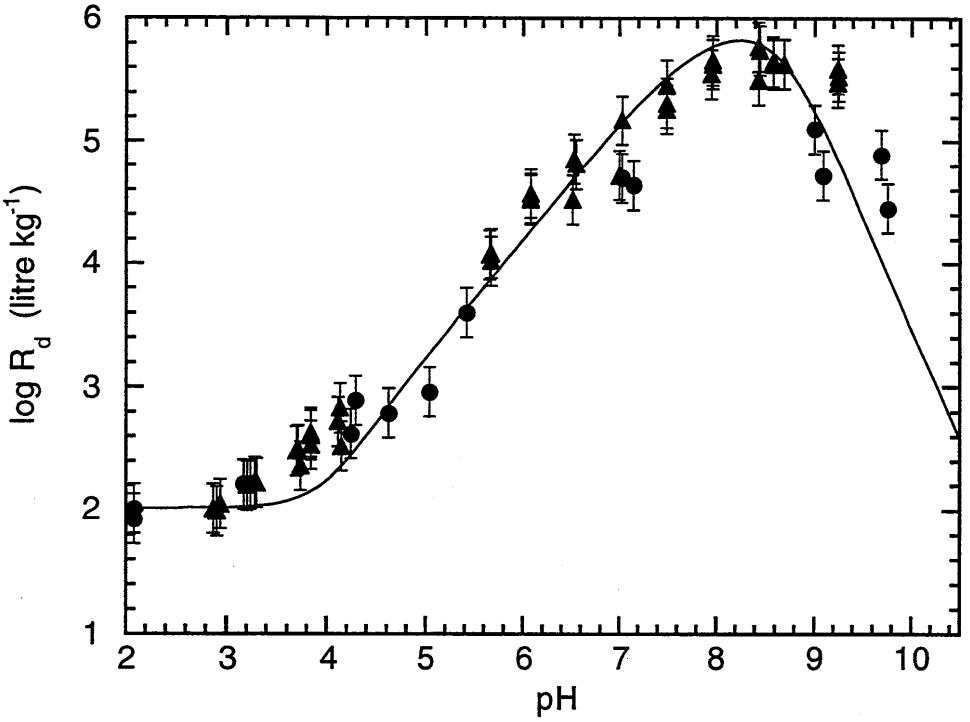

FIG. 10: Zn sorption edge on conditioned Na-montmorillonite in 0.1 M $NaClO_4$. The continuous line is a fit to the data using the 2SPNE-Model.
Fixed parameters: Zn inventory: 10^{-3} mol kg^{-1}; See Tables 1 and 3
Fitted parameter: log $^{S}K_{int}$ (Zn) = 1.6

9.3 Zinc Isotherms

For fits to the isotherm data, the only free parameter in the model is the SC constant for the weak sites. In principle two types of weak sites are available (see sections 7.5) and therefore two different constants could be used to fit the data. However, as discussed in the previous chapter, acid/base constants play an important role in determining where sorption on a certain set of sites becomes important. From the acid/base constants for $\equiv S^{W2}OH$ type sites (log $K_{int}(+)$ =6, log $K_{int}(-)$ = -10.5) we are able to infer that any potential contribution to sorption is only likely to be made at high pH values. (See for example section 12.2 and the discussion concerning the sorption of Mg and Ca in the next section.) The experimental data show that Zn sorption occurs predominantly in the pH range from ~ 3 to ~ 9, Figure 10. Consequently, to a first approximation the contribution of $\equiv S^{W2}OH$ type sites to the sorption of Zn is neglected. This is

also in accord with our overall philosophy of trying to keep the model as simple as possible and to keep the number of parameters to a minimum.

Two sets of isotherm data were measured for Zn at pH values of 5.6 and 7. A value for the Zn surface complexation constant for the weak sites, $^{W1}K_{int}(Zn)$, was duly fitted to the sorption results for pH = 5.6, Figure 11.

Since all the parameters describing Zn sorption on conditioned Na-montmorillonite are now fixed, a first test for the model was to compare the Zn sorption isotherm calculated at pH = 7 with the experimental measurements. This comparison is presented in Figure 12. Although the model predicts slightly more sorption in the higher concentration range (equilibrium Zn concentrations greater than approximately 5×10^{-5} M) the overall correspondence between calculated and measured data is good. Attempts to optimise the $^{W1}K_{int}(Zn)$ value using both sets of data brought little or no further improvement in the fits. However, in general terms, it is clearly advantageous if this parameter can be fitted and optimised over two isotherms measured at different pH values. A summary of the parameter data set used to fit the Zn sorption measurements is given in Table 4.

A further point worthy of note from Figure 11 is that the Zn-Na selectivity coefficient, calculated from the sorption edge at trace Zn concentrations, Figure 10, appears to be valid at the highest concentrations measured where the cation exchange mechanism is dominant. At an equilibrium concentration of $\sim 10^{-3}$ M the Zn is occupying ~25% of the available cation exchange sites. Thus, the Zn-Na selectivity coefficient value of 3.9 can be taken as being constant in the equivalent fractional occupancy range from near zero up to at least 0.25. This is in accord with the findings of MAES et al. (1976).

Table 4: Summary of surface complexation reactions and intrinsic constants for Zn sorption on conditioned Na-montmorillonite

Surface complexation reaction	Mass action equation	log K_{int}
$\equiv S^{S}OH + Zn^{2+} \Leftrightarrow \equiv S^{S}OZn^{+} + H^{+}$	$^{S}K_{int} = \frac{[\equiv S^{S}OZn^{+}]\cdot\{H^{+}\}}{[\equiv S^{S}OH]\cdot\{Zn^{2+}\}}$	1.6
$\equiv S^{W1}OH + Zn^{2+} \Leftrightarrow \equiv S^{W1}OZn^{+} + H^{+}$	$^{W1}K_{int} = \frac{[\equiv S^{W1}OZn^{+}]\cdot\{H^{+}\}}{[\equiv S^{W1}OH]\cdot\{Zn^{2+}\}}$	-2.7

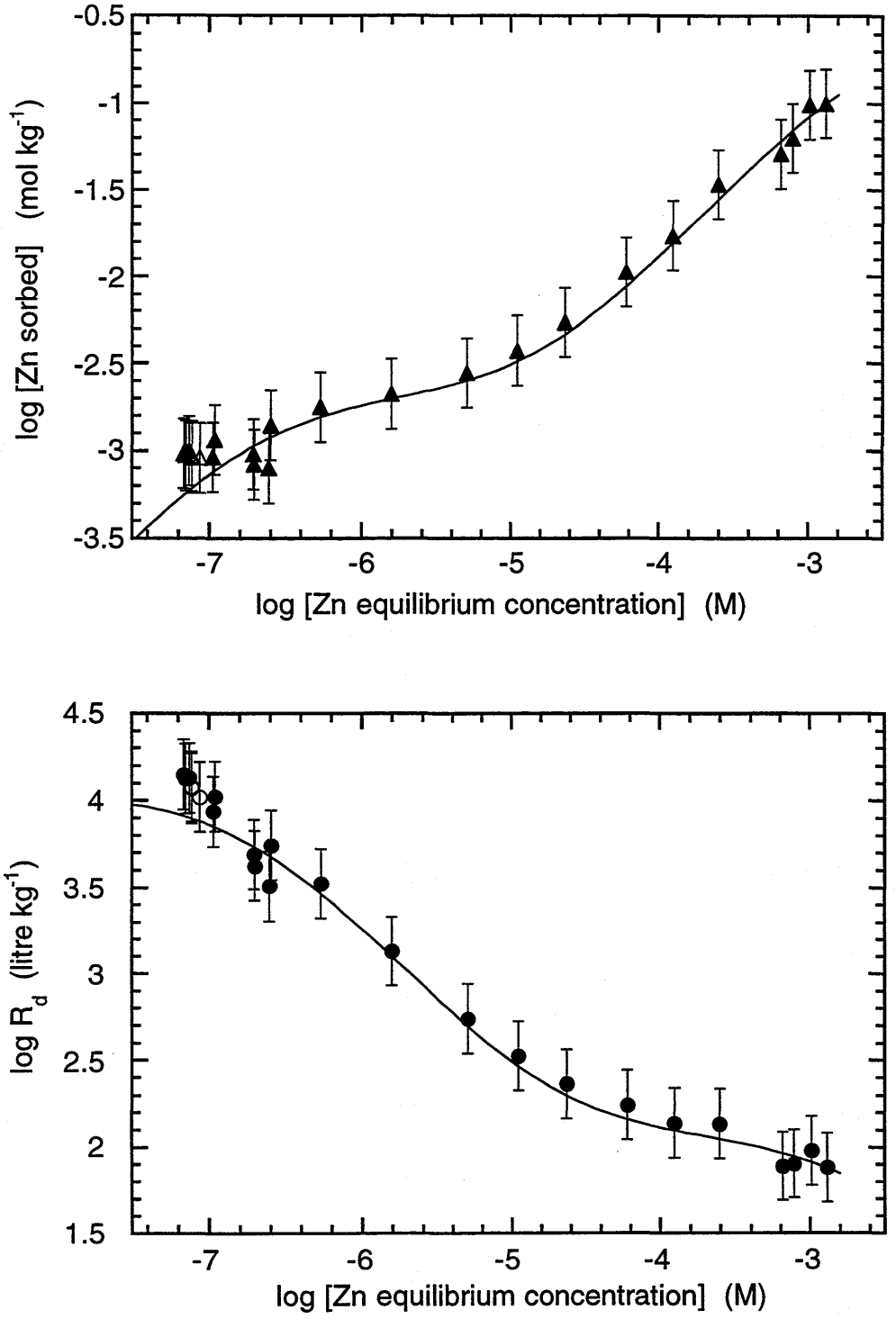

FIG. 11: Zn sorption on conditioned Na-montmorillonite in 0.1 M $NaClO_4$ at pH = 5.6
The continuous line is a fit to the data using the 2SPNE-Model.
Fixed parameters: See Tables 1 and 3; log $^{S}K_{int}$ (Zn) =1.6
Fitted parameter: log $^{W1}K_{int}$ (Zn) =-2.7

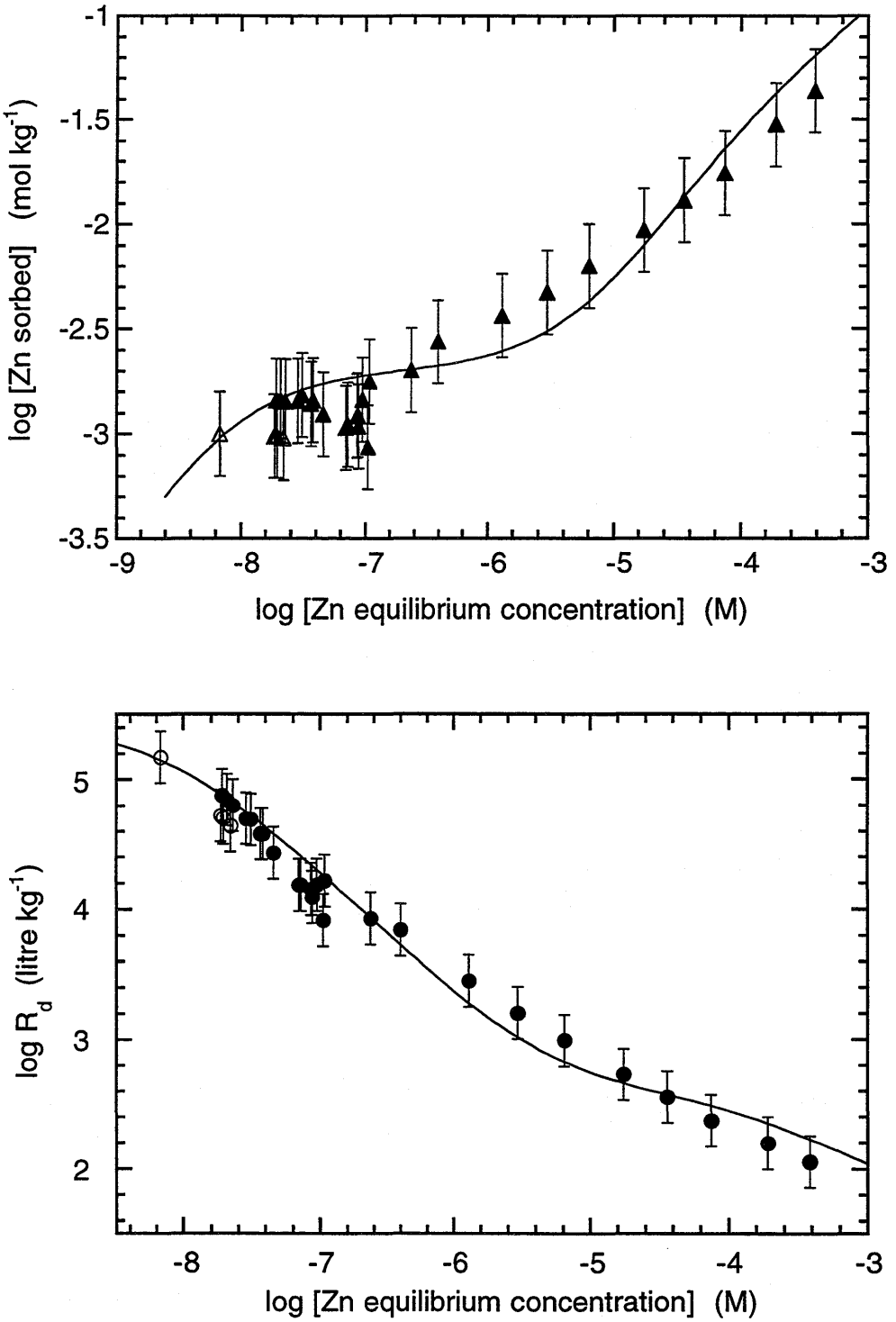

FIG. 12: Zn sorption on conditioned Na-montmorillonite in 0.1 M $NaClO_4$ at pH = 7
The continuous lines are calculated using the 2SPNE-model.
Fixed parameters: See Tables 1, 3 and 4
No Fit Parameters

10 "INACTIVE " SORPTION EDGES FOR Zn, Mg, Mn AND Ca.

10.1 General

In Part I it was concluded that Zn, Mn, Mg and Ca were present as sorbed cations on conditioned Na-montmorillonite at levels of ~ 10^{-3} (Zn), ~ 4 x 10^{-4} (Mn), 3-6 x 10^{-3} (Mg) and ~ 10^{-3} (Ca) mol kg^{-1}. These data, together with water chemistry measurements from batch titration experiments at 0.5 M $NaClO_4$, were used to deduce "inactive" sorption edges for the four elements as described in Part II, section 4.5. The errors in the data points given in Figures 13 (a), (b) and 14 (a), (b) are quite large. The reasons for this are discussed in Part II, section 4.5. The sorption behaviour of these cations is briefly examined here so that any possible competitive influences on the Ni sorption measurements can be assessed. Also, a first broad view of the surface complexation sorption characteristics of Mn, Mg and Ca is presented.

10.2 Zinc and Manganese

The sorption characteristics of Zn have already been examined in some detail and the continuous line in Figure 13(a) was calculated using the acid/base and intrinsic SC constants given previously. A comparison of the plot and measured data serves as an indicator of the sort of discrepancies existing between the data obtained using tracers and the rather more inaccurate data derived from "inactive" measurements. Similar uncertainties are to be expected for the other "inactive" sorption edges.

The best fit to the "inactive" Mn sorption edge was achieved with a log K_{int}(Mn) surface complexation constant of - 0.2 in the presence of a Zn inventory of 10^{-3} mol kg^{-1}. The shoulder on the Mn sorption edge curve shown in Figure 13 (b) at pH ~ 10 arises because Zn hydrolysis reactions in the aqueous phase are beginning to reduce the quantities of Zn sorbed on the $\equiv S^SOH$ type sites, thereby releasing sites upon which Mn can sorb and hence increasing Mn sorption. The aqueous hydrolysis of Mn only begins to affect its sorption at pH values well above 10.

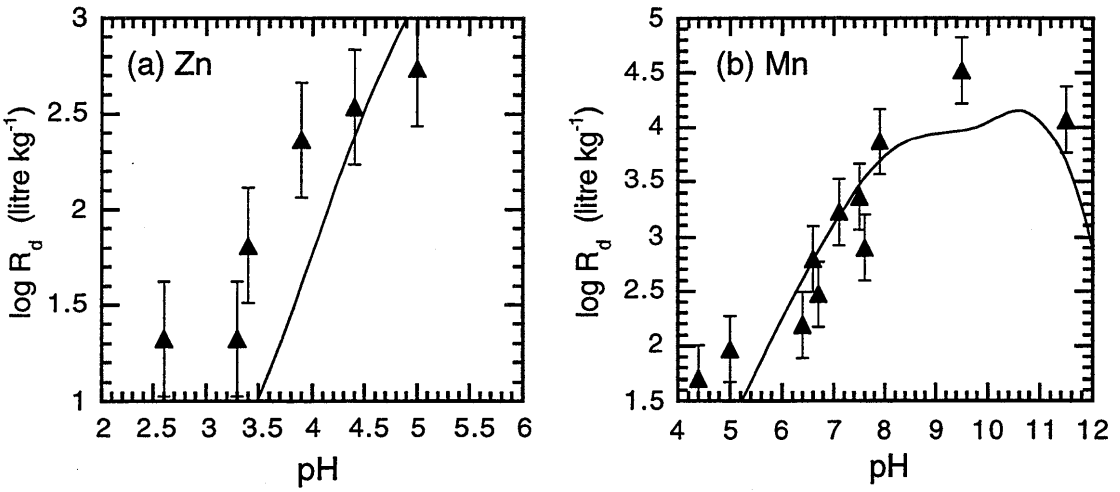

FIG. 13: "Inactive" sorption edges for (a) Zn and (b) Mn.
(a) Zn: The continuous line was calculated using the 2SPNE-model with all parameters fixed (Tables 1, 3 and 4).
The Zn inventory was fixed at 10^{-3} mol kg^{-1}
(b) Mn: The continuous line is a fit to the data using the 2SPNE-model.
Fixed parameters: see Tables 1, 3 and 4. Mn inventory = 4 x 10^{-4} mol kg^{-1}
Fitted parameter: log $^{S}K_{int}$ (Mn) = -0.2

Comparison of the sorption edges for Mn, Figure 13(b), and Ni, Figure 16, indicates that their SC sorption behaviour is similar and this similarity is of course reflected in their strong site SC constants. The data available imply that there may be some competitive effects from Mn on the sorption of Ni, and that Mn should be included in the analysis of the Ni data. It should however be recognised that the SC constant for Mn on the $\equiv S^{S}OH$ sites was deduced from experimental data having relatively large uncertainties, and therefore can only be considered to be an estimate.

10.3 Magnesium and Calcium

The inactive sorption edges for Mg and Ca are given in Figures 14 (a) and (b) respectively where it can be clearly seen that sorption by surface complexation only begins to become important at relatively high pH values, ~ 8.5 for Mg and ~ 9.5 for Ca. Additional sorption edge measurements for calcium were made as a function of $NaClO_4$ concentration using ^{45}Ca as tracer. These results are shown in Figure 15.

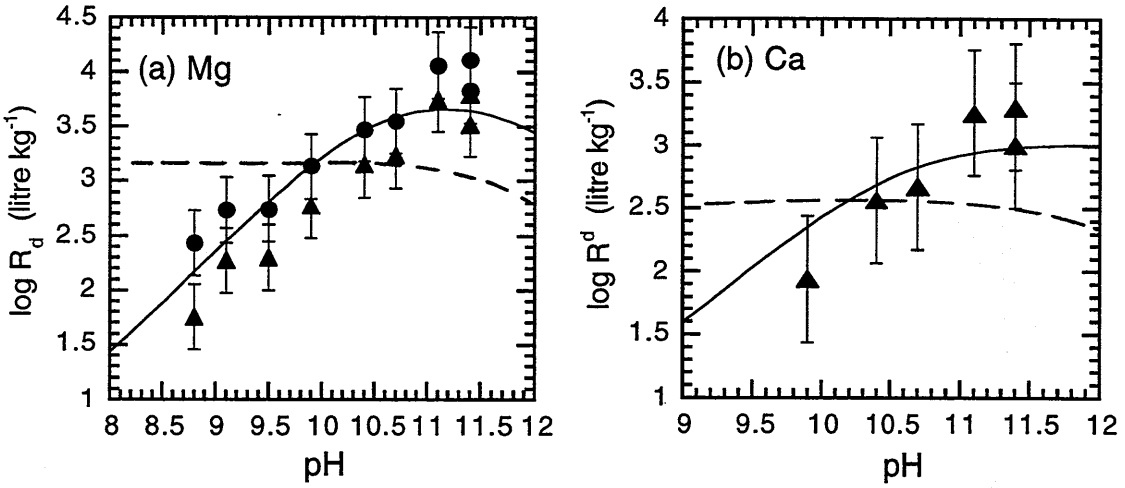

FIG. 14: "Inactive" sorption edges for (a) Mg and (b) Ca

The continuous lines are fits to the data using the 2SPNE-model.

Fixed parameters: See Tables 1, 3 and 4. Mg inventory: 3 - 6 x 10^{-3} mol kg^{-1}

Ca inventory: 10^{-3} mol kg^{-1}

Fitted parameters: (a) Mg; log $^{W2}K_{int}$ (Mg) = -4.7

(b) Ca; log $^{W2}K_{int}$ (Ca) = -5.5

The dashed lines are attempted fits to the sorption data using $\equiv S^{W1}OH$ type sites. (For details see text.)

The observation that both cations exhibit broad sorption peaks at pH values greater than 10.5, Figure 14, indicates that the pKa for the deprotonation of the sites responsible must also be roughly of this magnitude. Mainly for this reason these data are interpreted as indicating that sorption is most likely to be occurring on $\equiv S^{W2}OH$ sites rather than on $\equiv S^{W1}OH$ type sites. Note that for the dashed lines in Figures 14 (a) and 14 (b) which represent attempts to fit the sorption of Mg and Ca on the $\equiv S^{W1}OH$ type sites, the only adjustable parameter is the surface complexation constant on the weak sites and varying this merely moves the whole curve up or down but does not change its slope in these pH ranges.

A fitting exercise showed that the Mg and Ca edges could not be satisfactorily reproduced using either $\equiv S^{S}OH$ plus $\equiv S^{W1}OH$ sites, or $\equiv S^{W1}OH$ sites alone. Fits could be achieved using $\equiv S^{W1}OH$ plus $\equiv S^{W2}OH$ sites, but an almost equally good correspondence with the measured data was achieved using only the $\equiv S^{W2}OH$ sites. The quality of the measured data for the "inactive" sorption edges do not merit a more thorough fitting exercise. We see the fit to the data achieved using the $\equiv S^{W2}OH$ sites, shown in Figures 14 (a) and (b) and 15, as

only the first step in describing the sorption behaviour of Mg and Ca. Because of their sorption characteristics, Mg and Ca are highly unlikely to be competitive with Ni and therefore do not need to be considered in the analysis of the Ni sorption data.

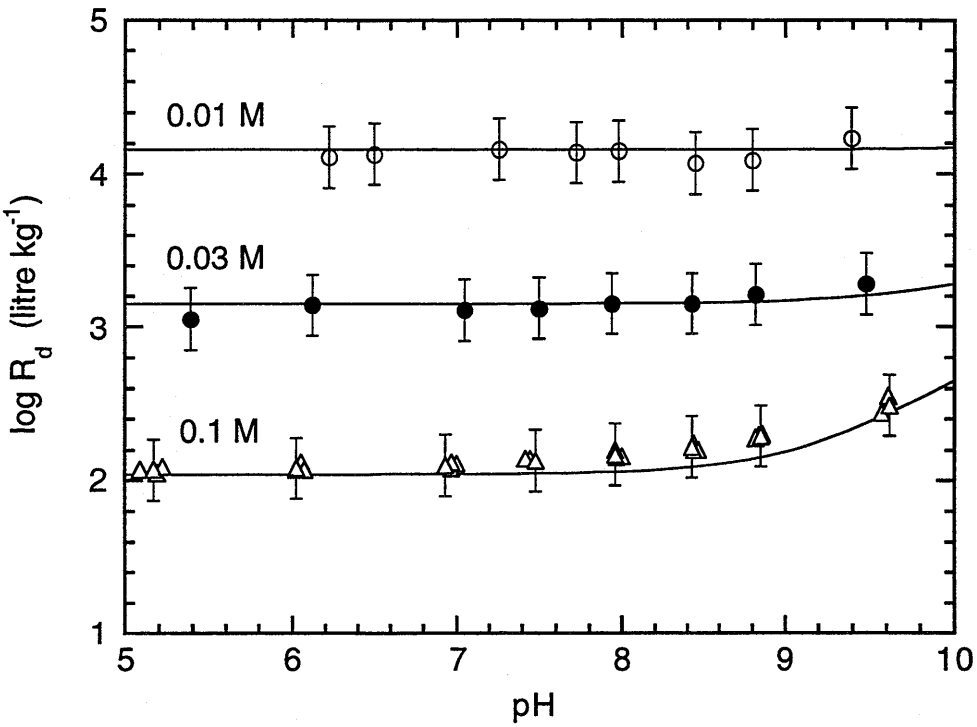

FIG. 15: Ca sorption edges on conditioned Na-montmorillonite measured at 0.1 M (Δ), 0.03 M (●) and 0.01 M (O) $NaClO_4$.
The continuous lines are calculated using the 2SPNE-model with all parameters fixed (See Tables 1,3 and 4; log $^{W2}K_{int}$ (Ca) = -5.5). The Ca inventory was fixed at 10^{-3} mol kg^{-1}.

Table 5: Summary of surface complexation reactions, intrinsic constants and inventories for Mn, Mg and Ca sorption on conditioned Na-montmorillonite.

Surface complexation reaction	Mass action equation	log K_{int}	Inventory (mol kg^{-1})
$\equiv S^{S}OH + Mn^{2+} \Leftrightarrow \equiv S^{S}OMn^{+} + H^{+}$	${}^{S}K_{int} = \frac{[\equiv S^{S}OMn^{+}]\cdot\{H^{+}\}}{[\equiv S^{S}OH]\cdot\{Mn^{2+}\}}$	-0.2	4×10^{-4}
$\equiv S^{W2}OH + Mg^{2+} \Leftrightarrow \equiv S^{W2}OMg^{+} + H^{+}$	${}^{W2}K_{int} = \frac{[\equiv S^{W2}OMg^{+}]\cdot\{H^{+}\}}{[\equiv S^{W2}OH]\cdot\{Mg^{2+}\}}$	-4.7	$3\text{-}6 \times 10^{-3}$
$\equiv S^{W2}OH + Ca^{2+} \Leftrightarrow \equiv S^{W2}OCa^{+} + H^{+}$	${}^{W2}K_{int} = \frac{[\equiv S^{W2}OCa^{+}]\cdot\{H^{+}\}}{[\equiv S^{W2}OH]\cdot\{Ca^{2+}\}}$	-5.5	10^{-3}

11 NICKEL SORPTION

11.1 Nickel Sorption Edges

Nickel sorption edge measurements at three $NaClO_4$ concentrations (0.1, 0.03 and 0.01 M) are presented in Figures 16-18.

In previous sections it was argued that the background impurity cations Zn and Mn, with inventories of ~ 10^{-3} mol kg^{-1} and ~ 4×10^{-4} mol kg^{-1} respectively, were competitive with Ni at trace concentrations for sorption on the $\equiv S^SOH$ sites. This requires that Zn and Mn inventory values, together with their respective intrinsic surface complexation constants on the $\equiv S^SOH$ sites, must be included in the calculations of Ni sorption edges. The list of fixed parameters used in MINSORB for the Ni sorption edges, and subsequently for the Ni isotherm data, are those given in Tables 1, 3, 4 and 5.

A SC constant for Ni on the strong sites was then fitted for the Ni sorption edge at 0.1 M $NaClO_4$ using the same procedures as described previously. The continuous line in Figure 16 gives the best fit obtained using a value for log $^SK_{int}(Ni)$ of -0.1.

With all parameters now determined, MINSORB was used to calculate the sorption edges at 0.03 and 0.01 M $NaClO_4$ which are shown by the continuous lines in Figures 17 and 18. A summary of the data and calculations are given in Figure 19. The calculated values at 0.01 and 0.03 M represent first tests of the validity of the model and model parameters under conditions other than those at which the parameters were determined. The correspondence between calculated and measured values is good.

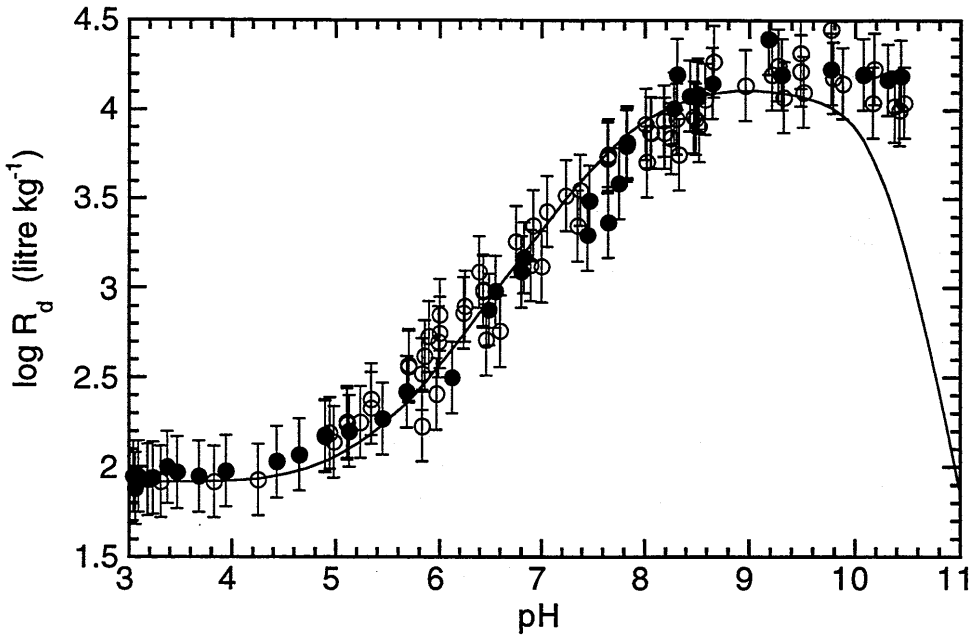

FIG. 16: Ni sorption edge on conditioned Na-montmorillonite in 0.1 M $NaClO_4$. The continuous line is a fit to the data using the 2SPNE model taking into account the Zn and Mn inventories together with their respective SC constants on the $\equiv S^SOH$ sites.

Fixed parameters: See Tables 1, 3, 4 and 5.

Fit parameter: log $^SK_{int}$ (Ni) = -0.1

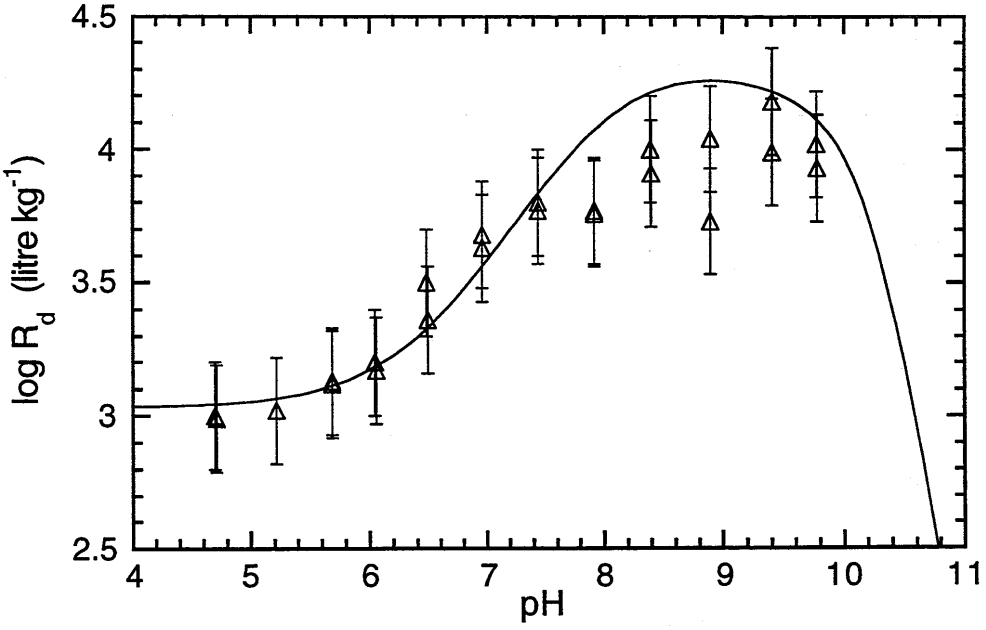

FIG. 17: Ni sorption edge on conditioned Na-montmorillonite in 0.03 M $NaClO_4$. The continuous line is calculated using the 2SPNE-model with all parameters fixed. See Tables 1, 3, 4, 5 and log $^SK_{int}$ (Ni) = -0.1

No fit parameters.

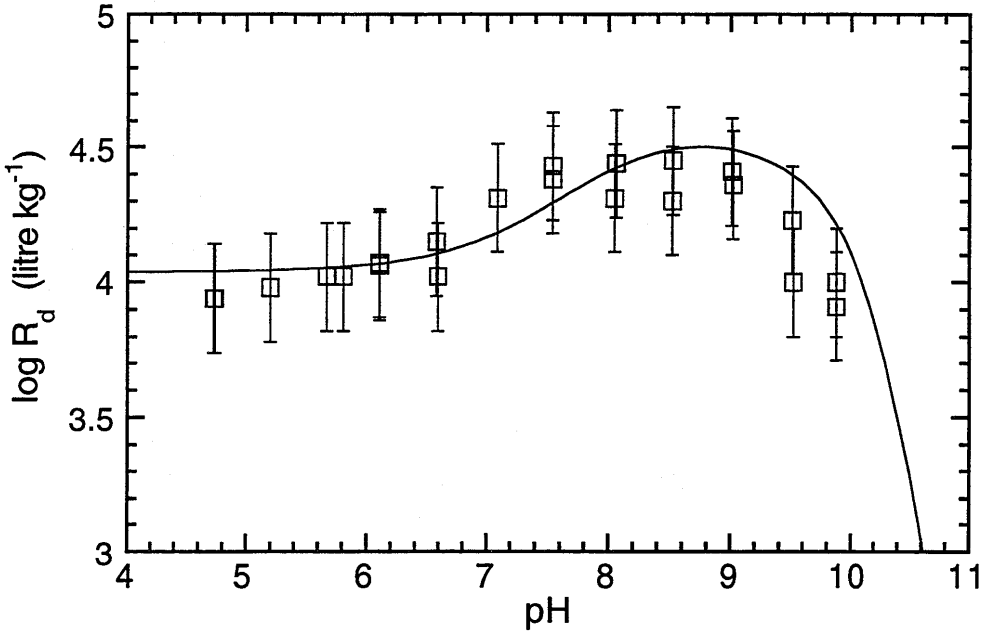

FIG. 18: Ni sorption edge on conditioned Na-montmorillonite in 0.01 M $NaClO_4$. The continuous line is calculated using the 2SPNE model with all parameters fixed. See Tables 1, 3, 4, 5 and log $^{S}K_{int}$ (Ni) = -0.1
No fit parameters.

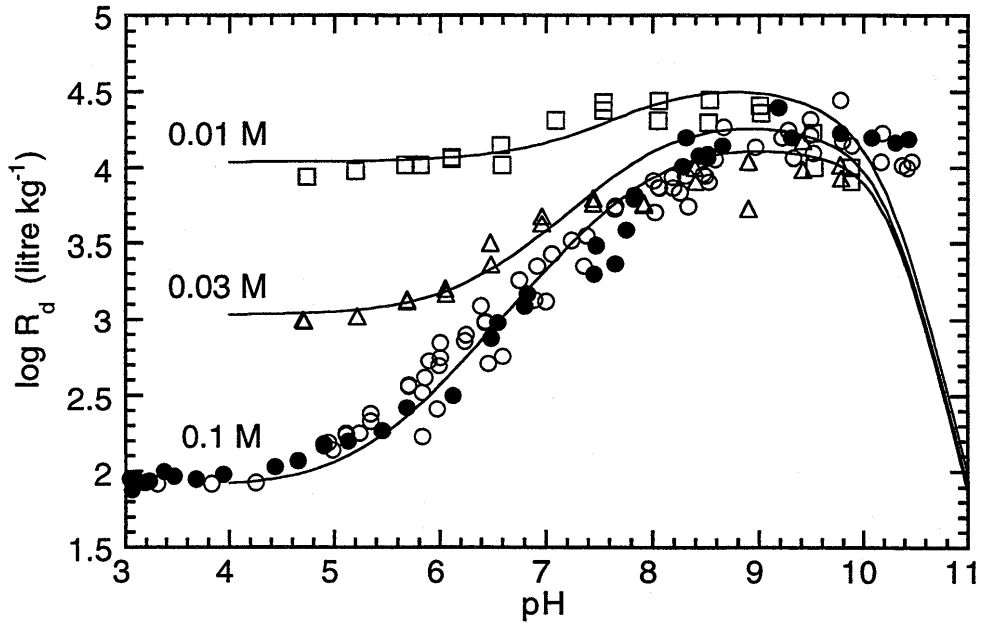

FIG. 19: Experimental data and modelled curves for Ni edges on conditioned Na-montmorillonite at 0.1 M (O,●); 0.03 M (Δ) and 0.01 M (❑) $NaClO_4$

11.2 Nickel Sorption Isotherms

Sorption isotherms for Ni were measured at 6 different pH values between 4.7 and 8.2 over equilibrium concentration ranges extending from approximately 10^{-9} M to 10^{-4} M, Figures 20 to 25.

Only one parameter in the model describing Ni sorption on conditioned Na-montmorillonite remains unknown at this stage, namely the intrinsic surface complexation constant for $\equiv S^{W1}OH$ site types. A value of log $^{W1}K_{int}(Ni)$ of -3.1 was determined on a best fit basis for the isotherm at pH = 8.2 given in Figure 20. The continuous lines given in Figures 21 to 25 are isotherms calculated with no free fit parameters and, in analogy with the Ni sorption edge data, represent tests of the validity of the model and the associated model parameter values.

A summary of the surface complexation reactions and the intrinsic constants for Ni is given in Table 6.

Table 6: Summary of surface complexation reactions and intrinsic constants for Ni sorption on conditioned Na-montmorillonite

Surface complexation reaction	Mass action equation	log K_{int}
$\equiv S^{S}OH + Ni^{2+} \Leftrightarrow \equiv S^{S}ONi^{+} + H^{+}$	$^{S}K_{int} = \frac{[\equiv S^{S}ONi^{+}]\cdot\{H^{+}\}}{[\equiv S^{S}OH]\cdot\{Ni^{2+}\}}$	-0.1
$\equiv S^{W1}OH + Ni^{2+} \Leftrightarrow \equiv S^{W1}ONi^{+} + H^{+}$	$^{W1}K_{int} = \frac{[\equiv S^{W1}ONi^{+}]\cdot\{H^{+}\}}{[\equiv S^{W1}OH]\cdot\{Ni^{2+}\}}$	-3.1

Finally, in an analogous manner to Zn, we note that the Ni-Na selectivity coefficient determined at trace Ni concentrations ($N_{Ni} < 0.001$) is also valid at relatively high Ni equilibrium concentrations (~ 5 x 10^{-4} M), Figure 20, corresponding to an equivalent fractional cation occupancy of ~ 0.04.

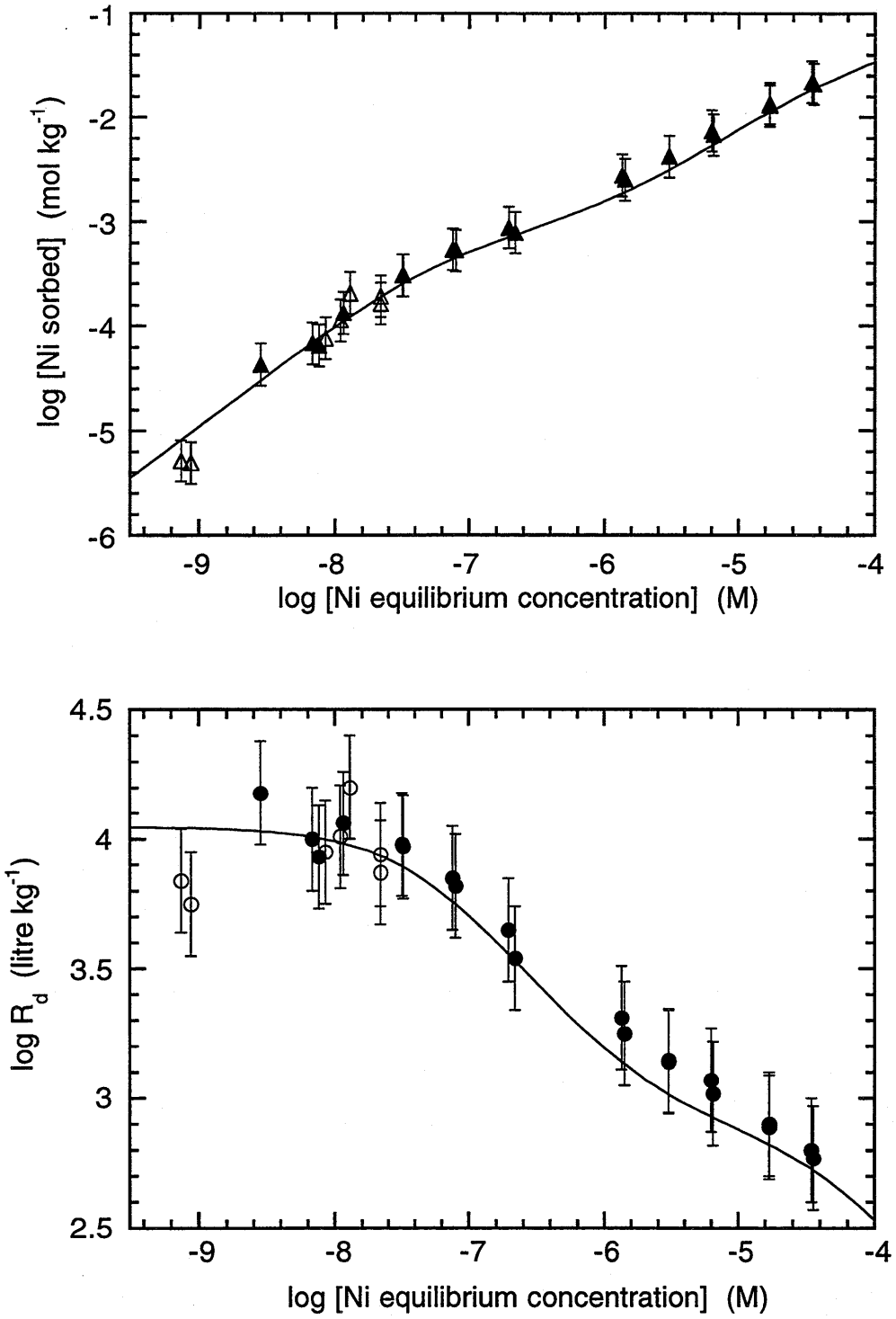

FIG. 20: Ni sorption isotherm on conditioned Na-montmorillonite in 0.1 M $NaClO_4$ at pH = 8.2

The continuous line is a fit to the data using the 2SPNE-model.

Fixed parameters: See Tables 1, 3, 4,5 and log $^{S}K_{int}$ (Ni) = -0.1

Fit parameter: log $^{W1}K_{int}$ (Ni) = -3.1

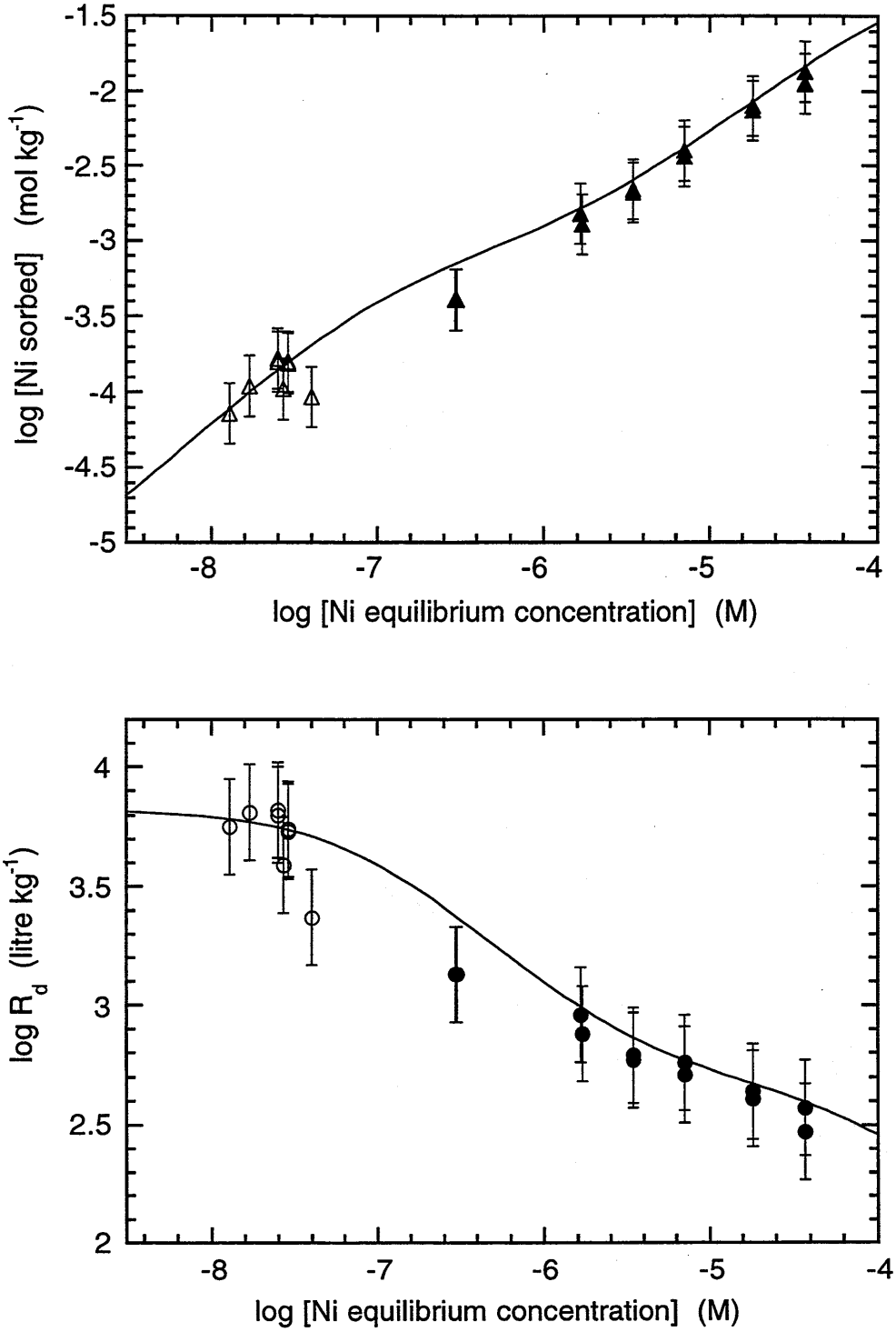

FIG. 21: Ni sorption isotherm on conditioned Na-montmorillonite in 0.1 M $NaClO_4$ at pH = 7.7

The continuous lines are calculated using the 2SPNE-model.

Fixed parameters: See Tables 1, 3, 4, 5 and 6

No fit parameters

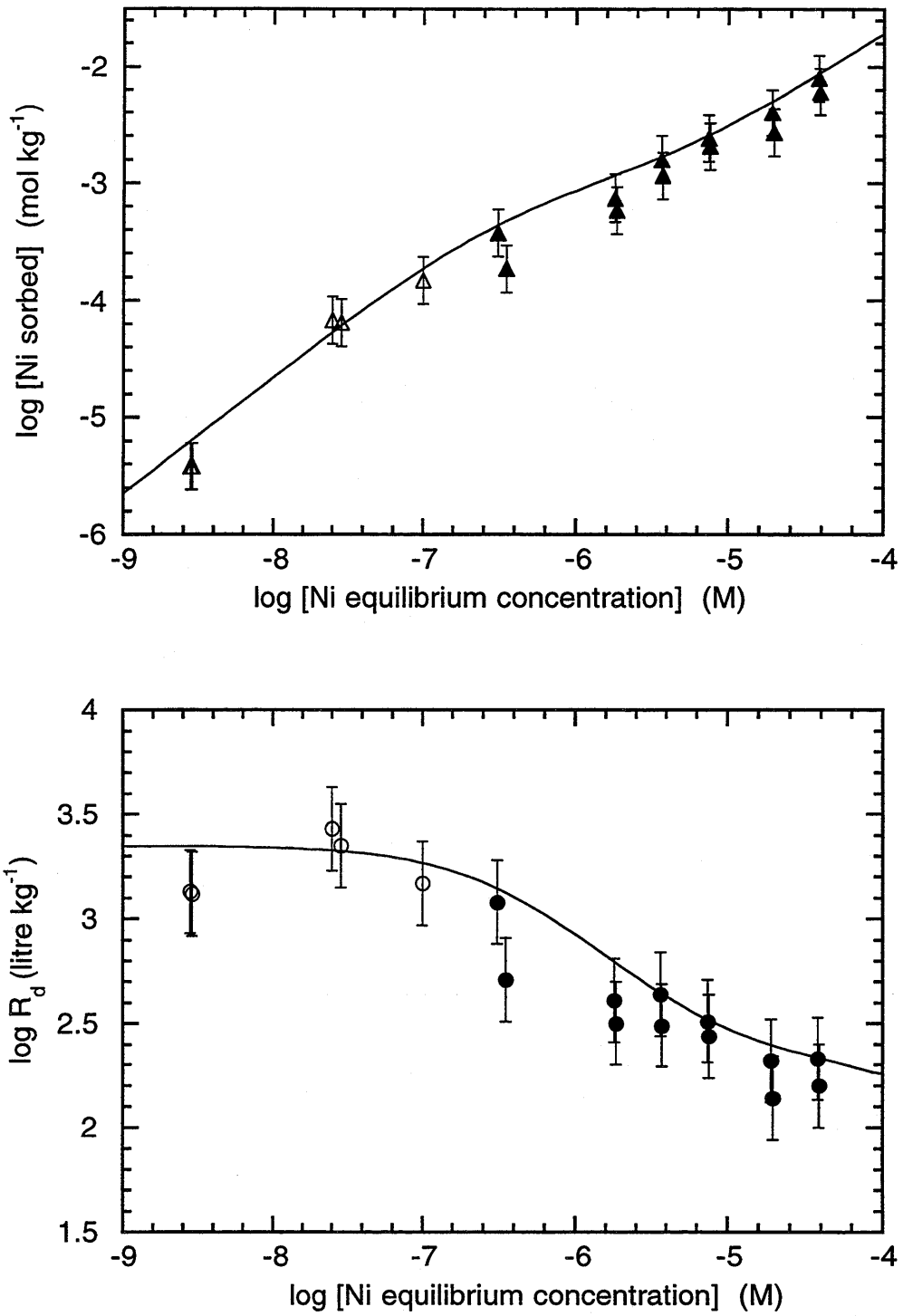

FIG. 22: Ni sorption isotherm on conditioned Na-montmorillonite in 0.1 M $NaClO_4$ at pH = 7.0

The continuous lines are calculated using the 2SPNE-model.

Fixed parameters: See Tables 1, 3, 4, 5 and 6

No fit parameters

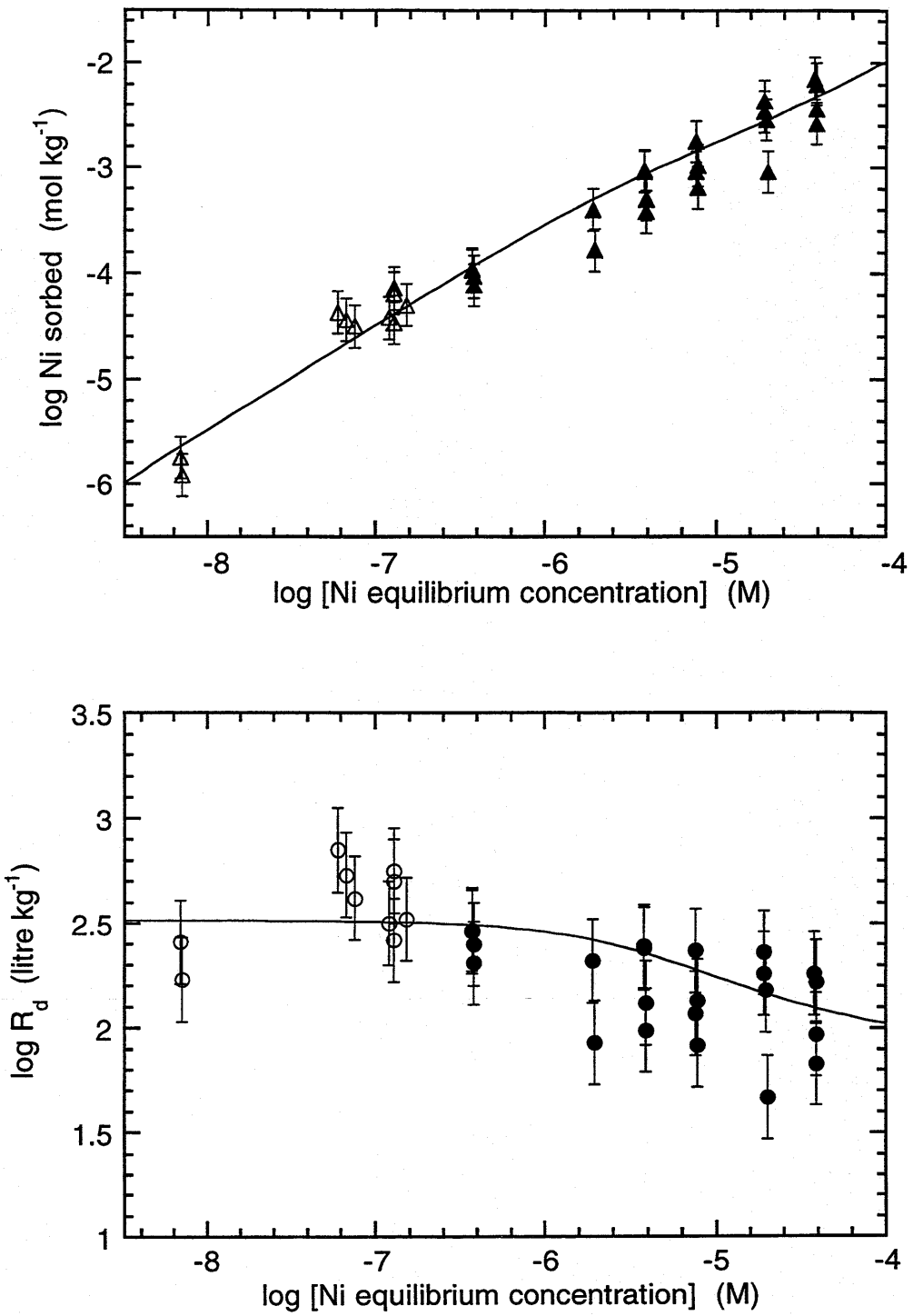

FIG. 23: Ni sorption isotherm on conditioned Na-montmorillonite in 0.1 M $NaClO_4$ at pH = 5.9

The continuous lines are calculated using the 2SPNE-model.

Fixed parameters: See Tables 1, 3, 4, 5 and 6

No fit parameters

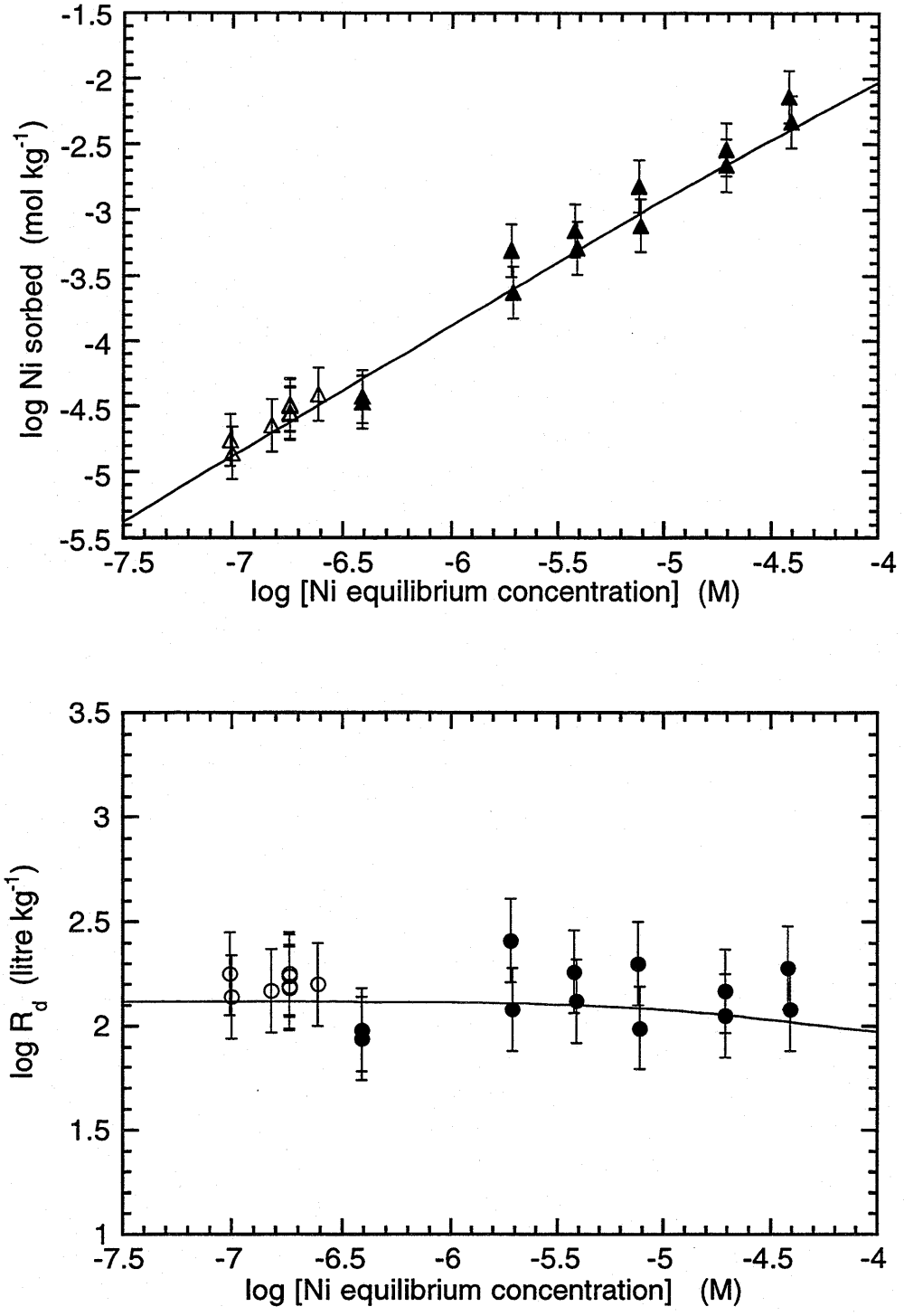

FIG. 24: Ni sorption isotherm on conditioned Na-montmorillonite in 0.1 M $NaClO_4$ at pH = 5.1

The continuous lines are calculated using the 2SPNE-model.

Fixed parameters: See Tables 1, 3, 4, 5 and 6

No fit parameters

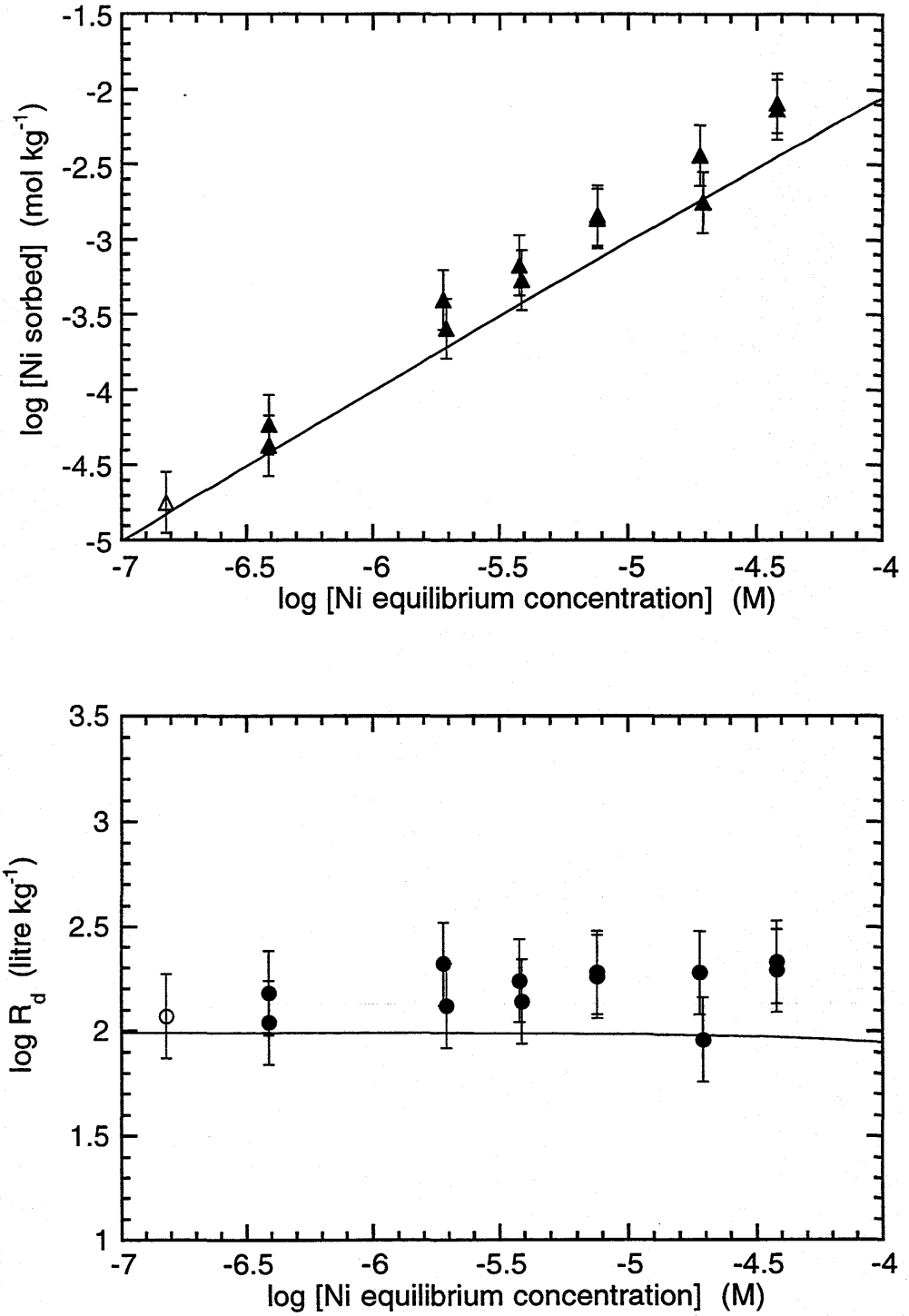

FIG. 25: Ni sorption isotherm on conditioned Na-montmorillonite in 0.1 M $NaClO_4$ at pH = 4.7

The continuous lines are calculated using the 2SPNE-model.

Fixed parameters: See Tables 1, 3, 4, 5 and 6

No fit parameters

12 THE 2SPNE-MODEL: EXAMPLES OF SURFACE SPECIATION

12.1 Model Summary

Through a series of fitting stages carried out for titration and sorption edge data it was clearly demonstrated that a non-electrostatic model provided the best description of the measurements on conditioned Na-montmorillonite. The model contained two protolysis site types, $\equiv S^{W1}OH$ and $\equiv S^{W2}OH$, with different capacities and acid/base constants and was hence referred to as a two site protolysis non electrostatic model - abbreviated to 2SPNE-model.

Because $\equiv S^{W2}OH$ sites deprotonated at such high pH values (see following section), the sorption of Zn and Ni on the weak site types occurred exclusively on the $\equiv S^{W1}OH$ sites. A set of high affinity sites, $\equiv S^{S}OH$, with a relatively low capacity, was predominantly responsible for the uptake of nuclides at low concentrations.

In general, two sorption mechanisms, cation exchange and surface complexation, were required to describe the uptake of Zn and Ni by Na-montmorillonite. These mechanisms were characterised in terms of site capacities, selectivity coefficients and surface complexation constants. In the tables below, the sorption reactions occurring on the various site types, together with the corresponding mass action equations and constants determined in this work, are summarised.

In the following, we would like to illustrate the model by briefly examining the protolysis, sorption edge and sorption isotherm characteristics of Na-montmorillonite from a slightly different aspect to that presented previously. By calculating the surface speciation, we can break down the overall observed behaviour and view it in terms of the component parts. For example, the uptake of radionuclides by the different individual site types and how this varies with the experimental conditions can be used to illustrate and explain the general characteristics of sorption isotherms. In this way a better insight into, and understanding of, sorption processes and the way they interact with one another, can be gained.

Table 7: Summary of cation exchange reactions and selectivity coefficients for Zn-Na, Ni-Na and Ca-Na equilibria on conditioned Na-montmorillonite.

Cation exchange reaction	Mass action equation	K_C
$2Na-Clay+Zn^{2+} \Leftrightarrow Zn-Clay + 2Na^{+}$	$K_C(Zn-Na) = \frac{(N_{Zn}) \cdot \{Na^{+}\}^2}{(N_{Na})^2 \cdot \{Zn^{2+}\}}$	3.9
$2Na-Clay+Ni^{2+} \Leftrightarrow Ni-Clay + 2Na^{+}$	$K_C(Ni-Na) = \frac{(N_{Ni}) \cdot \{Na^{+}\}^2}{(N_{Na})^2 \cdot \{Ni^{2+}\}}$	3.1
$2Na-Clay+Ca^{2+} \Leftrightarrow Ca-Clay + 2Na^{+}$	$K_C(Ca-Na) = \frac{(N_{Ca}) \cdot \{Na^{+}\}^2}{(N_{Na})^2 \cdot \{Ca^{2+}\}}$	4.1
Cation exchange capacity:	8.7×10^{-1} eq. kg^{-1}	

Note: N_M = equivalent fractional occupancy (see Chapter 5, Part II)

Table 8: Summary of site types, site capacities, and protolysis constants for conditioned Na-montmorillonite.

Site types:	Site capacities:	
$\equiv S^{S}OH$	2.0×10^{-3} moles kg^{-1}	
$\equiv S^{W1}OH$	4.0×10^{-2} moles kg^{-1}	
$\equiv S^{W2}OH$	4.0×10^{-2} moles kg^{-1}	
Surface complexation reaction	**Mass action equation**	**log K_{int}**
$\equiv S^{S}OH + H^{+} \Leftrightarrow \equiv S^{S}OH_2^{+}$	$K_{int}(+) = \frac{[\equiv S^{S}OH_2^{+}]}{[\equiv S^{S}OH] \cdot \{H^{+}\}}$	4.5
$\equiv S^{S}OH \Leftrightarrow \equiv S^{S}O^{-} + H^{+}$	$K_{int}(-) = \frac{[\equiv S^{S}O^{-}] \cdot \{H^{+}\}}{[\equiv S^{S}OH]}$	-7.9
$\equiv S^{W1}OH + H^{+} \Leftrightarrow \equiv S^{W1}OH_2^{+}$	$K_{int}(+) = \frac{[\equiv S^{W1}OH_2^{+}]}{[\equiv S^{W1}OH] \cdot \{H^{+}\}}$	4.5
$\equiv S^{W1}OH \Leftrightarrow \equiv S^{W1}O^{-} + H^{+}$	$K_{int}(-) = \frac{[\equiv S^{W1}O^{-}] \cdot \{H^{+}\}}{[\equiv S^{W1}OH]}$	-7.9
$\equiv S^{W2}OH + H^{+} \Leftrightarrow \equiv S^{W2}OH_2^{+}$	$K_{int}(+) = \frac{[\equiv S^{W2}OH_2^{+}]}{[\equiv S^{W2}OH] \cdot \{H^{+}\}}$	6.0
$\equiv S^{W2}OH \Leftrightarrow \equiv S^{W2}O^{-} + H^{+}$	$K_{int}(-) = \frac{[\equiv S^{W2}O^{-}] \cdot \{H^{+}\}}{[\equiv S^{W2}OH]}$	-10.5

Table 9: Summary of cation surface complexation reactions and intrinsic constants for Zn, Ni, Mn, Ca and Mg on conditioned Na-montmorillonite. Inventory data for Zn, Mn, Ca and Mg are also given.

Surface complexation reaction	Mass action equation	log K_{int}
$\equiv S^S OH + Zn^{2+} \Leftrightarrow \equiv S^S OZn^+ + H^+$	${}^{S}K_{int} = \frac{[\equiv S^S OZn^+]\cdot\{H^+\}}{[\equiv S^S OH]\cdot\{Zn^{2+}\}}$	1.6
$\equiv S^S OH + Ni^{2+} \Leftrightarrow \equiv S^S ONi^+ + H^+$	${}^{S}K_{int} = \frac{[\equiv S^S ONi^+]\cdot\{H^+\}}{[\equiv S^S OH]\cdot\{Ni^{2+}\}}$	-0.1
$\equiv S^S OH + Mn^{2+} \Leftrightarrow \equiv S^S OMn^+ + H^+$	${}^{S}K_{int} = \frac{[\equiv S^S OMn^+]\cdot\{H^+\}}{[\equiv S^S OH]\cdot\{Mn^{2+}\}}$	-0.2
$\equiv S^{W1} OH + Zn^{2+} \Leftrightarrow \equiv S^{W1} OZn^+ + H^+$	${}^{W1}K_{int} = \frac{[\equiv S^{W1} OZn^+]\cdot\{H^+\}}{[\equiv S^{W1} OH]\cdot\{Zn^{2+}\}}$	-2.7
$\equiv S^{W1} OH + Ni^{2+} \Leftrightarrow \equiv S^{W1} ONi^+ + H^+$	${}^{W1}K_{int} = \frac{[\equiv S^{W1} ONi^+]\cdot\{H^+\}}{[\equiv S^{W1} OH]\cdot\{Ni^{2+}\}}$	-3.1
$\equiv S^{W2} OH + Mg^{2+} \Leftrightarrow \equiv S^{W2} OMg^+ + H^+$	${}^{W2}K_{int} = \frac{[\equiv S^{W2} OMg^+]\cdot\{H^+\}}{[\equiv S^{W2} OH]\cdot\{Mg^{2+}\}}$	-4.7
$\equiv S^{W2} OH + Ca^{2+} \Leftrightarrow \equiv S^{W2} OCa^+ + H^+$	${}^{W2}K_{int} = \frac{[\equiv S^{W2} OCa^+]\cdot\{H^+\}}{[\equiv S^{W2} OH]\cdot\{Ca^{2+}\}}$	-5.5

Intrinsic metal inventories:	
Zn:	10^{-3} mol kg^{-1}
Mn:	4×10^{-4} mol kg^{-1}
Ca:	10^{-3} mol kg^{-1}
Mg:	$3 - 6 \times 10^{-3}$ mol kg^{-1}

12.2 Surface Site Protonation and Deprotonation

Using the 2SPNE model and the acid/base constants and site capacities listed in Table 8, the contributions of the two protolysis site types $\equiv S^{W1}OH$ and $\equiv S^{W2}OH$ to the overall titration behaviour of conditioned Na-montmorillonite are shown in Figure 26. The results from a more detailed calculation illustrating the surface speciation of these 2 sites as a function of pH are presented in Figures 27 (a) and 27 (b).

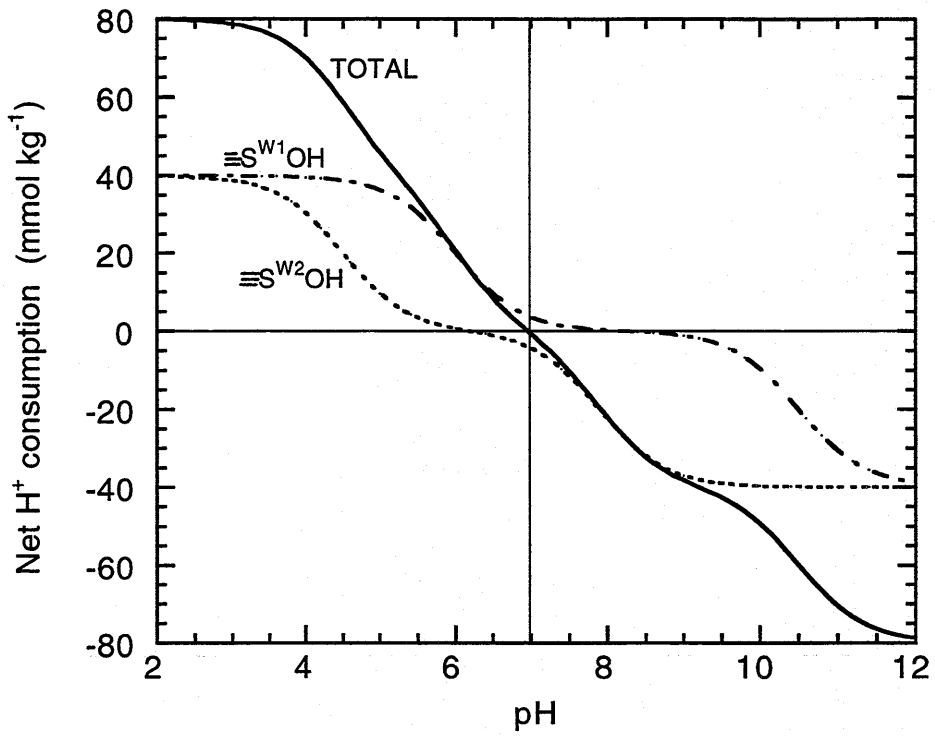

FIG. 26: Calculation of the net proton consumption of the two protolysis sites ($\equiv S^{W1}OH$ and $\equiv S^{W2}OH$) and the total net proton consumption as a function of pH.

The $pK_a(-)$ value for the $\equiv S^{W1}OH$ sites, Figure 27 (a), is approximately 8. At pH values above 8 the dominant surface species are the deprotonated sites, $\equiv S^{W1}O^-$, whose concentration remains constant. If the sorption edge measurements for Zn and Ni in Figures 10 and 16 respectively are examined, it can be readily appreciated that the peak sorption values also occur at a pH of approximately 8.

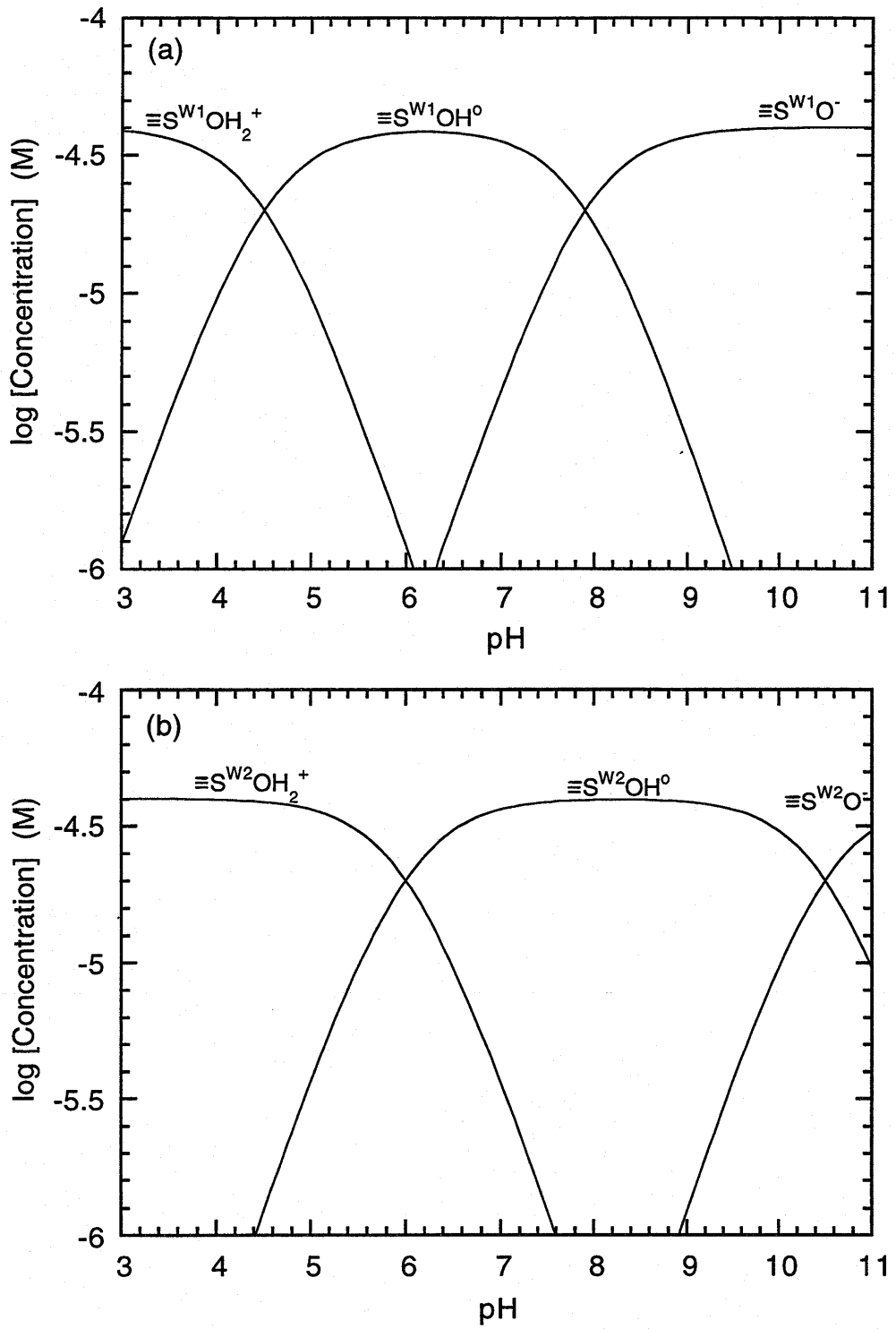

FIG. 27: Calculated surface speciation of the two protolysis sites for conditioned Na-montmorillonite as a function of pH at 0.1 M $NaClO_4$. (S:L = 1 gram $litre^{-1}$)
(a) $\equiv S^{W1}OH$
(b) $\equiv S^{W2}OH$

In the absence of hydrolysis, or any other complexation reactions, the sorption from pH = 8 onwards would remain constant since the $\equiv S^{W1}O^-$ concentration is virtually constant. The extent of the constant sorption region (plateau) is determined here by the hydrolysis behaviour of Ni and Zn. For Ni, the plateau is a prominent feature of the sorption edge. Hydrolysis does not begin to influence sorption until a pH of ~10. (The first hydrolysis constant for $Ni(OH)^+$ is $\sim 10^{-9.9}$.) For Zn, on the other hand, the sorption plateau is almost absent since the formation of mono-hydroxy species, with a first hydrolysis constant for $Zn(OH)^+$ of $\sim 10^{-8.9}$, begins to reduce the sorption almost as soon as the peak value is reached. As mentioned in section 7.2.2, the protolysis characteristics of the sorption sites are the main factor determining the position of the sorption edge.

12.3 Zn Sorption Edges

For the purposes of illustrating the characteristics of the model with respect to calculated sorption edges and isotherms, we have chosen Zn, with the additional condition that the system is initially Zn free.

The Zn sorption edge plots given in Figure 28 are made up of components from two sorption mechanisms. The first is cation exchange on the permanent charge sites, CE-Zn, and the second is surface complexation on the strong sites, $\equiv S^SOZn^+$. Figures 28 (a) and 28 (b) show their relative contributions at $NaClO_4$ background electrolyte concentrations of 0.1 and 0.01 M respectively.

The Zn-Na cation exchange contribution to the overall Zn sorption is very sensitive to the background electrolyte concentration and, in this particular system, varies as the inverse square of the $NaClO_4$ concentration, see for example Chapter 5 in Part II. In contrast, the influence of ionic strength on surface complexation reactions is insignificant. Thus the contribution of Zn uptake on the $\equiv S^SOH$ sites remains the same in both cases. The dominant sorption mechanism for Zn uptake on Na-montmorillonite at trace concentrations is sensitively dependent on the aqueous chemistry. Low pH and low ionic strength tend to favour cation exchange and whereas the reverse is true for surface complexation. At trace Zn concentration levels both of these mechanisms lead to linear sorption behaviour, but with different magnitudes.

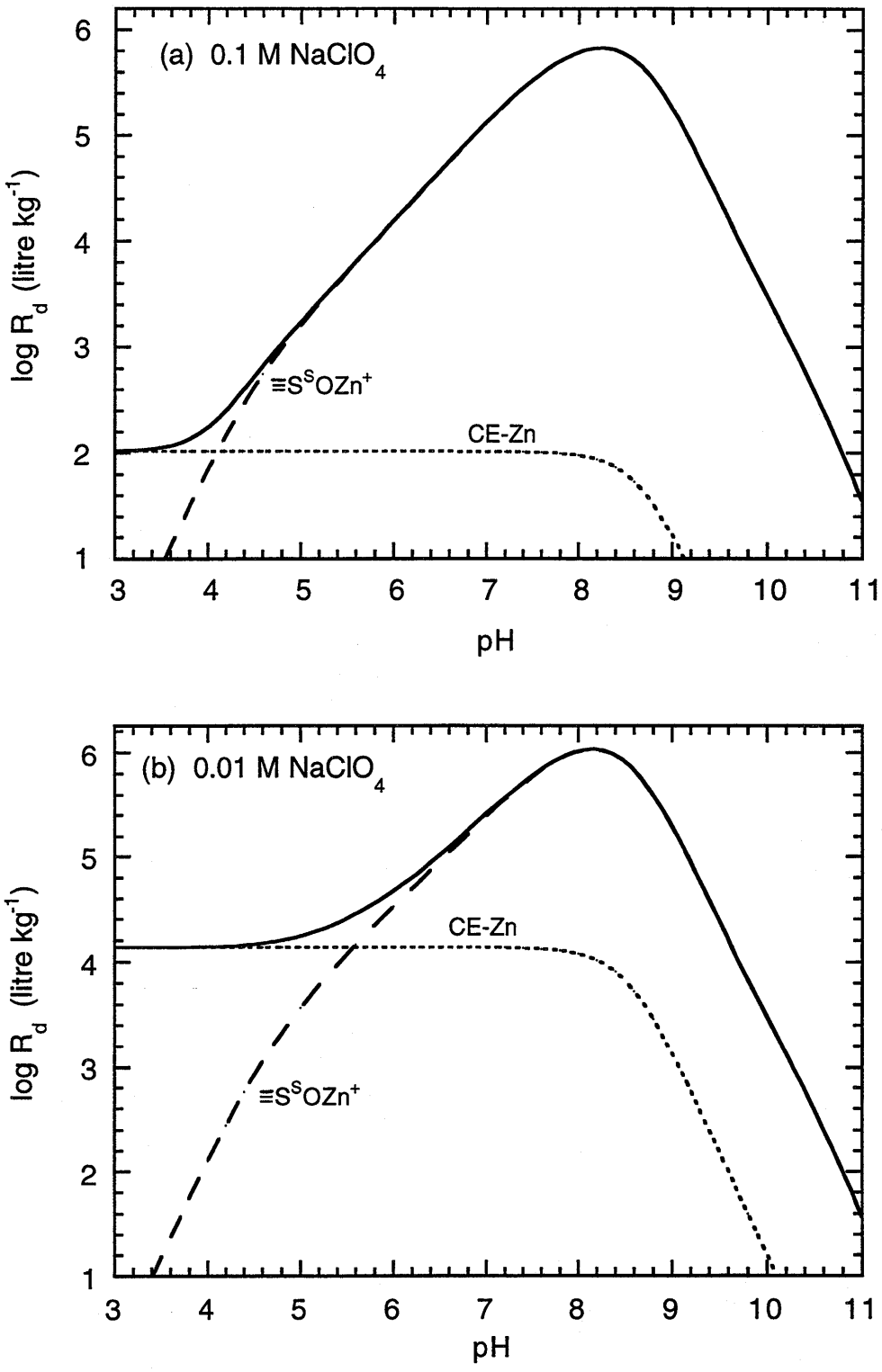

FIG. 28: Calculated sorption edges for Zn on conditioned Na-montmorillonite at an initial Zn concentration of 10^{-6} M. (S:L ratio = 1 gram litre^{-1})

(a) 0.1 M $NaClO_4$.

(b) 0.01 M $NaClO_4$.

Figure 29 illustrates the effect on the sorption edge of increasing the initial Zn concentration in the range from 10^{-8} to 10^{-5} M for a fixed S:L ratio of 1 gram litre $^{-1}$, and a background electrolyte concentration of 0.1 M $NaClO_4$.

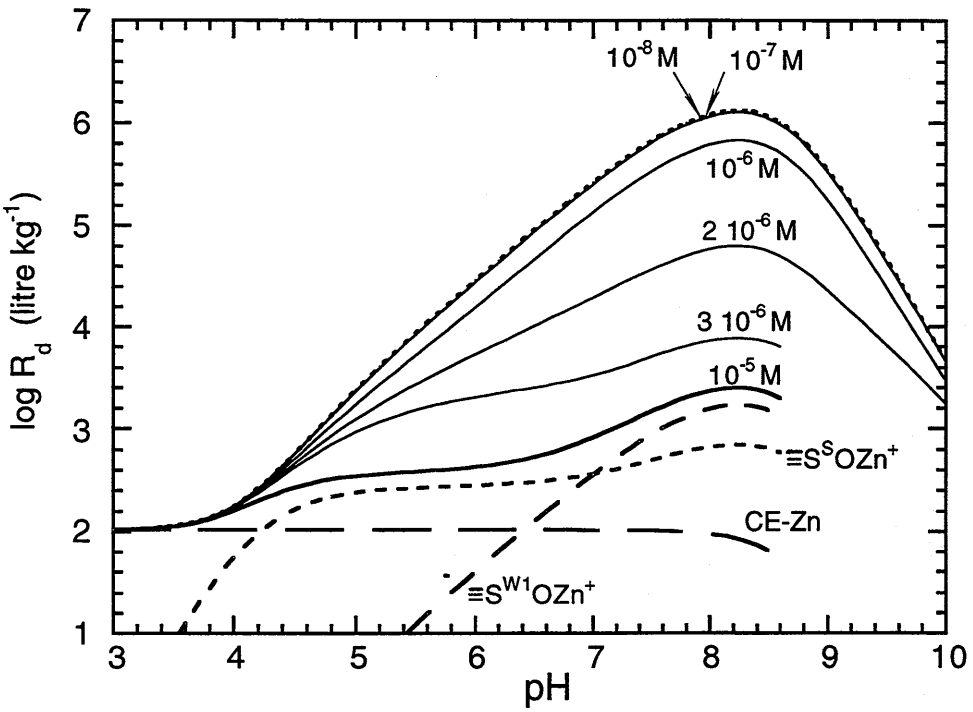

FIG. 29: Sorption edges for Zn on conditioned Na-montmorillonite at 0.1 M $NaClO_4$ as a function of initial Zn concentrations. (S:L ratio = 1 gram litre $^{-1}$). The contribution of the different surface species to the overall sorption is illustrated for the case where the initial concentration of Zn is 10^{-5} M.

Important here is not the initial Zn concentration or the S:L ratio per se, but rather the relationship between the Zn inventory and the quantity of strong sites available. For Zn inventories well below the strong site capacity of conditioned Na-montmorillonite (2 x 10^{-3} mol kg^{-1}), the sorption edge is independent of the inventory. (See the results of the calculations for Zn concentrations of 10^{-8} and 10^{-7} M in Figure 29.) However, the nearer the initial Zn concentration approaches the strong site concentration (≡S^SOH site capacity x S/L), the closer these sites become to being saturated and the larger is the reduction in sorption and the greater the effect on the form of the curve. This can be clearly seen in Figure 28 by comparing the changes in the curves between 10^{-8} and 10^{-6} and between 10^{-6} and 2 x 10^{-6} M Zn. At Zn concentrations greater than 2 x 10^{-6} M the strong sites are saturated and sorption begins to take place on the weak sites, ≡S^{W1}OH. However, the surface complexation constant for

these sites is considerably smaller than the constant for the strong sites, so their effect only becomes apparent at higher concentrations, 10^{-5} M Zn curve. Because of this the sorption falls rapidly for Zn inventories which are slightly larger than the quantity of strong sites available. (Compare the sorption edges for 2×10^{-6} and 3×10^{-6} M Zn.) The obvious consequence of this for the determination of surface complexation constants on the strong sites from experimentally determined sorption edges is that the experimental conditions must be chosen such that the inventory of the radionuclide in question should be very much less than the quantity of strong sites available. (See comments in section 5.2.) In addition, it should also be clear from these calculations that radionuclide sorption at trace concentrations can be significantly influenced by trace levels of background metal impurities also sorbing on the strong sites.

12.4 Zn Isotherms

The form of the sorption isotherm is strongly dependent on the experimental conditions which basically determine which sorption mechanism and which set(s) of sorption sites are contributing to the overall sorption. The shape of isotherms, shown as either log R_d versus log [equilibrium aqueous metal concentration] or log [moles of metal sorbed per kg] versus log [equilibrium aqueous metal concentration], can be relatively complex. The reason an isotherm has a particular form under particular conditions and how this form changes with changing conditions can be best appreciated by viewing the surface speciation of the sorbed nuclide. We have tried to illustrate this in the examples given in Figures 30 and 31.

The sorption isotherms for Zn can exhibit up to four distinct regions depending on the experimental conditions. Taking as an example Figure 30, it can be seen that at low Zn equilibrium concentrations sorption is only occurring on the $\equiv S^SOH$ type sites and consequently the sorption is linear (Region I). With increasing Zn concentration the strong sites are gradually saturated. Because the complexation constant for the weak sites is relatively low, there is a Zn concentration region where the strong sites are saturated and the weak sites are making no significant contribution to the sorption. Increasing Zn concentrations do not in this case lead to any increase in sorption. This shows itself as a plateau in Figure 30 (a) i.e. the quantity of Zn sorbed is constant, or in the R_d plot as a distribution ratio which is decreasing as the inverse of the equilibrium concentration, Region II.

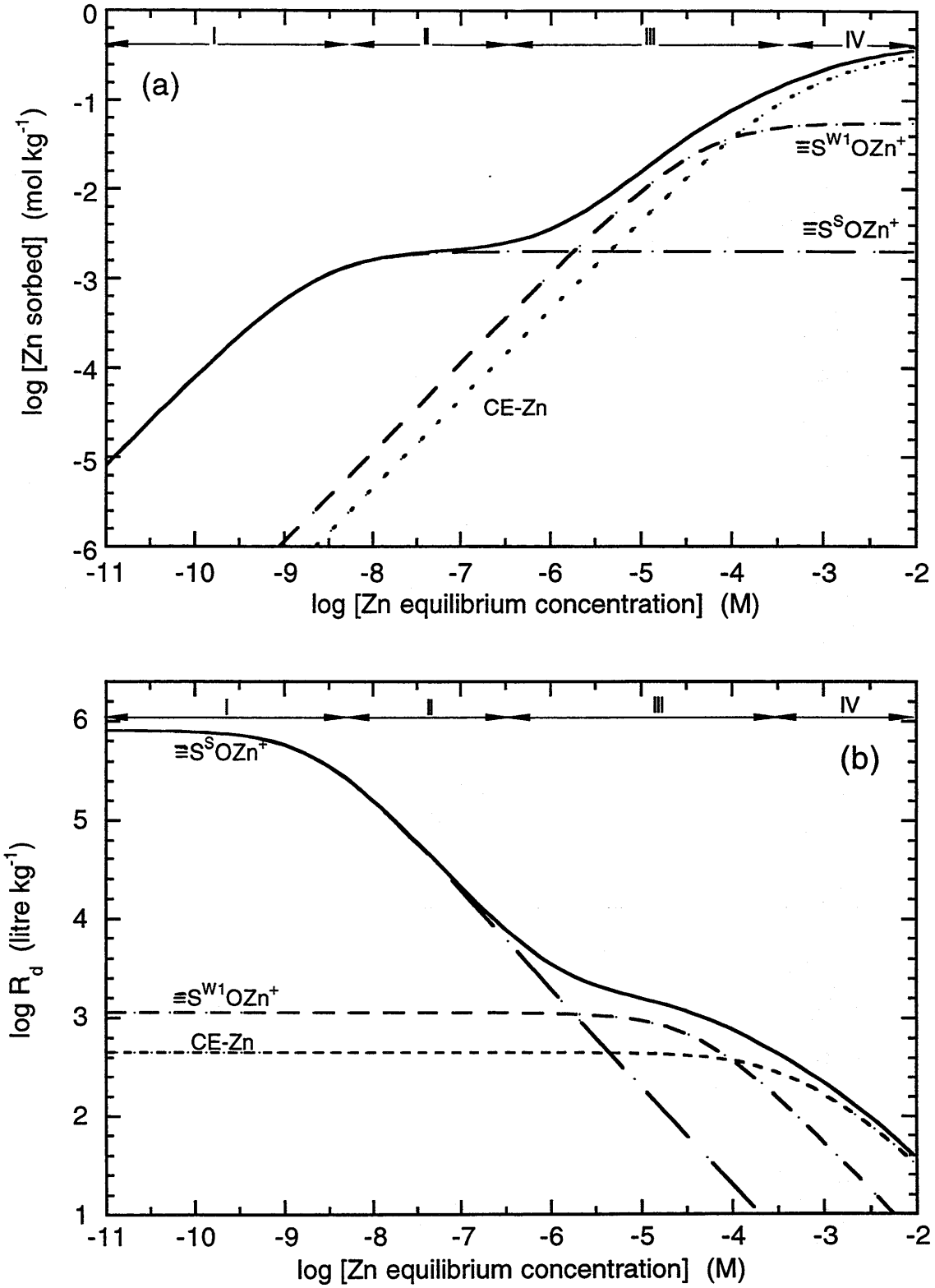

FIG. 30: Calculated sorption isotherms for Zn on Na-montmorillonite at pH = 7.5, illustrating the contribution of the different surface species to the overall sorption. ($NaClO_4 = 5 \times 10^{-2}$ M)

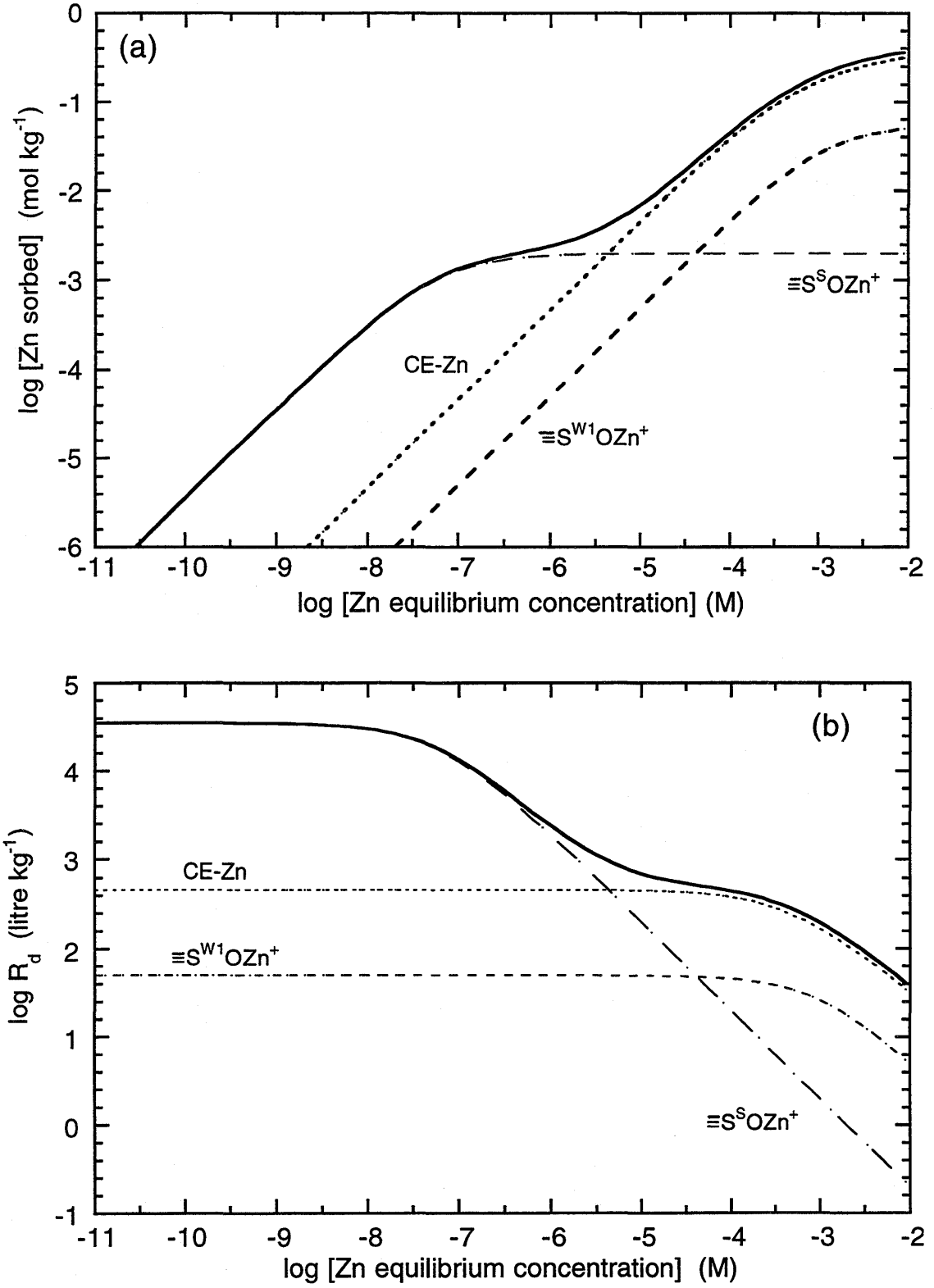

FIG. 31: Calculated sorption isotherms for Zn on Na-montmorillonite at pH = 6, illustrating the contribution of the different surface species to the overall sorption. ($NaClO_4 = 5 \times 10^{-2}$ M)

The cation exchange mechanism has been operating throughout this concentration range but only as a minor contributor to the total sorption. As the equilibrium Zn concentration increases still further, uptake on all three site types becomes comparable and combine together to produce a non-linear sorption behaviour, Region III. In Figure 30 this Freundlich type sorption behaviour extends for Zn equilibrium concentrations between 10^{-6} and 10^{-3} M. Finally, in the fourth region the sorption is dominated by cation exchange reactions. On this basis a linear type sorption behaviour might be expected. However, the onset of this region normally starts at such high Zn equilibrium concentrations that either, it is not reached at all because of solubility constraints, or the exchange sites are approaching saturation and the sorption behaviour is similar to that in Region II, i.e. the R_d tends to decrease as the inverse of the Zn concentration.

The plot in Figure 31 was calculated for pH = 6, but otherwise under the same conditions as for Figure 30. At this pH the two main sorption sites are the $\equiv S^SOH$ and the cation exchange sites. The form of the curve has changed in certain significant respects. In particular, the plateau region in Figure 31 (a) has almost completely disappeared and been replaced by a highly non-linear sorption region.

The sorption edge and isotherm calculations given above are a few selected examples which serve to illustrate the complexity of the interactions between sorbate, sorbent and water chemistry which combine together to produce the overall sorption.

13 "ELECTROSTATICS"

From a purely modelling point of view we have clearly demonstrated that an electrostatic term in the mass action equations describing protonation and deprotonation reactions and the sorption of bivalent cations on Na-montmorillonite is not needed for the range of experimental conditions investigated here. Simply put, using the diffuse double layer model as described in Chapter 4, we can model all the measured data without a coulombic term, but only a limited part of the data with a coulombic term. At the time of writing this report we have no physical explanation as to why the electrostatic term should be absent or, alternatively, why its influence is so small that it can be neglected. Nevertheless, it might be worthwhile to briefly explore a few directions in which explanations might be sought.

One of the major differences between clay minerals and oxides is that the surface charge of the former may not only determined by the acid/base characteristics of the ≡SOH type edge sites but also by a fixed permanent negative surface charge, equivalent to the CEC, arising from isomorphous substitutions in the clay mineral lattice. A consequence of this would be that the overall electrical potential at the surface at any given pH should be treated as resulting from a combination of the charge from the pH dependent protonation/deprotonation behaviour of the ≡SOH sites, and the pH independent permanent negative charge. Also, since charge contributions from the whole clay mineral surface are being taken into consideration here, the total surface area of Na-montmorillonite (~7.5 x 10^5 m^2 kg^{-1}; VAN OLPHEN 1966) is the appropriate value to be used in the calculations.

In the conditioned Na-montmorillonite the permanent negative charge amounts to 8.7 x 10^{-1} equivalents kg^{-1}, whereas the maximum charge arising from the ≡SOH type sites is 8 x 10^{-2} equivalents kg^{-1}. Thus, on this concept for the origin of surface charge, the magnitude and sign are determined by the permanent charge, and are essentially fixed, except for a pH dependent perturbation from the ≡SOH type sites which amounts to a maximum of approximately ±10%. The net effect is that the magnitude of the electrostatic term remains almost constant as a function of pH.

We did make some efforts to model the data using the above concept together with two protolysis sites, and generally the fits achieved for titration and sorption

edge measurements looked quite promising. However, this version of the modified DDL model broke down when attempting to reproduce Ni sorption edges measured as a function of $NaClO_4$ concentration, Figures 16 to 19. Experimentally there was only a very weak dependency of sorption on ionic strength at higher pH values whereas the model predicted a very strong influence (Increases in sorption by more than one order of magnitude for a change in $NaClO_4$ concentration from 0.1 to 0.01 M). The origin of the calculated dependency of sorption on ionic strength lies in the Gouy-Chapman relation from which the surface potential (Ψ) in the electrostatic term is obtained, see equations 1 to 8.

As soon as surface charge densities become moderately large ($> 10^{-2}$ coulombs per square metre), variations in ionic strength will have potentially significant influences on the magnitude of the electrostatic term and thereby on the sorption of species which form charged surface complexes. As stated above, this dependency arises from the Gouy-Chapman relation which is in-built into the version of the DDL-model use here. Since the DDL-model with electrostatics cannot reproduce the Ni sorption behaviour in Figures 16 to 19, then one possibility is that the Gouy-Chapman equation relating surface potential and charge is not appropriate for Na-montmorillonite.

If we stay with the Gouy-Chapman relation then we have to accept that modelled sorption values will be a function of ionic strength. However, it should be noted that the influence on sorption decreases when the values of surface charge densities remain small ($< 10^{-2}$ coulomb per square metre) over the ranges of ionic strengths typically used in experimental investigations, 0.5 to 0.005 M. Therefore, another potential explanation may be that the surface charge densities are low for all combinations of pH and ionic strengths used in the experiments. In the sorption edge measurements, radionuclide up take is on the small concentration of "strong sites" and it may be in the nature of these sites that their origin is different from the weak $\equiv$SOH type sites and that they are widely separated from one another, thus having low site densities.

One final possibility is that Ni forms a neutral surface complex in a total surface complexation reaction which involves the release of only one proton. We could find no chemically reasonable surface reactions fulfilling these criteria.

Non of the speculative ideas/suggestions given above provide in themselves an answer to the original question posed, and a physical explanation as to why "electrostatics" are not needed in the mass action equations remains an open question.

14 SUMMARY

Since many of the parameter values in surface complexation models cannot be determined directly, calibration of the model by fitting parameters to experimental data plays an integral role in any mechanistic approach to sorption. However, when the data base is small, there is the danger that the model and parameters fitted to a limited data set may not be generally applicable, even though the fit to the measurements may be good. For this reason the development of a model and the determination of the associated parameter sets which are applicable over a wide range of conditions requires a large experimental data base. Normally, such an experimental data base should consist of titration, sorption edge and sorption isotherm measurements as a function of variables such as pH, ionic strength and nuclide inventory.

We have developed and applied a modelling approach, summarised in Figure 1, Chapter 5, which involves a stepwise iterative process starting with titration data and then proceeding sequentially to sorption edge measurements and then to isotherm data. Wherever possible parameter values are deduced from experimental measurements. Fit parameter values obtained at any point in the calibration process are fixed for all subsequent steps. The aim is to find a consistent parameter set for the model which is capable of describing all the measured data. This procedure is illustrated in detail in all the calculations given from Chapter 7 onwards.

In attempts to derive parameter sets for the experimental data we were able to show that, although the diffuse double layer model for oxides provided a reasonable fit to the titration data, it failed to reproduce the sorption edge measurements. In particular, this model could not predict the correct slope to the rising edge, the overall shape of the curve and the position of the sorption maximum. These observations led us to conclude that an electrostatic term was not required in a SC-model for Na-montmorillonite. The DDL-model was accordingly modified and it was subsequently demonstrated that a two site protolysis model without electrostatics provided a good basis for describing the available data. This so-called 2SPNE-model was then used throughout the work.

At the conclusion to the model calculations for the titration data a basic parameter data set for Na-montmorillonite comprising of site capacities and surface protonation/deprotonation constants was determined. These parameters are intrinsic to the conditioned Na-montmorillonite and therefore independent of the sorbing species and/or experimental conditions. Consequently their values are invariant and were fixed in all of the calculations.

In the absence of experimental evidence to the contrary, the simplest surface complexation reaction for a bivalent metal was always chosen, equation 7. Given this reaction and a two site sorption model, the values of three parameters are required to define the sorption characteristics of a particular metal cation, namely, the strong site capacity, $\equiv S^SOH$, and the surface complexation constants for the strong, $^SK_{int}(M)$, and weak sites, $^{W1}K_{int}(M)$. The strong site capacity is often a fit parameter but we showed in Chapter 8 how a good estimate of its value can be obtained from experimental data. $^SK_{int}(M)$ is obtained as a fit parameter to the sorption edge data. The only remaining unknown is the surface complexation constant for the weak sites, $^{W1}K_{int}(M)$, and this is obtained from the sorption isotherm data.

In principle only one sorption edge and one sorption isotherm are required to determine the three parameters $\equiv S^SOH$, $^SK_{int}(M)$ and $^{W1}K_{int}(M)$. In practice, however, isotherms at more than one pH are useful since they can be used to check the parameter values.

In the conditioned Na-montmorillonite system Zn and Mn were present at specific levels as background impurities. Both of these cations can compete with Ni for the available sorption sites and thereby influence its sorption behaviour. Zn was investigated in detail and the appropriate surface complexation constants determined. For Mn only an estimate of the surface complexation constant for the strong sites could be made. In the analysis of the Ni data, the influence of both Zn and Mn was included in the calculations to determine the Ni surface complexation constants.

Although not directly the subject of this work, cation exchange reactions, which are very important in most clay systems, were included in all of the calculations. It should be realised that in many circumstances, such as low pH or high equilibrium metal concentrations or low ionic strength, cation exchange can be the dominant sorption mechanism.

ACKNOWLEDGEMENTS

Professor W. Stumm is warmly thanked for his critical and helpful comments on this work. Gratitude is expressed to Drs. U. Berner, E. Wieland and J. Hadermann (PSI) and Dr. I. Hagenlocher (Nagra) for the many interesting discussions and for reviewing the manuscript. Partial financial support was provided by Nagra.

REFERENCES

BAEYENS, B. & BRADBURY, M.H. (1995a): A quantitative mechanistic description of Zn, Ca and Ni sorption on Na-montmorillonite Part I: Physico-chemical characterisation and titration measurements. PSI Bericht Nr.95-10. Paul Scherrer Institut, Villigen, Switzerland and Nagra Technical Report NTB 95-04, Nagra, Wettingen, Switzerland.

BAEYENS, B. & BRADBURY, M.H. (1995a): A quantitative mechanistic description of Zn, Ca and Ni sorption on Na-montmorillonite Part II: Sorption measurements. PSI Bericht Nr. 95-11, Paul Scherrer Institut, Villigen, Switzerland and Nagra Technical Report NTB 95-05, Nagra, Wettingen, Switzerland.

BEENE, G.M., BRYANT, R. & WILLIAMS, D.J.A. (1991): Electrochemical properties of illites. J. Colloid Interface Sci. 147, 358-369.

BOLT, G.H. & VAN RIEMSDIJK, W.H. (1987): Surface chemical processes in soils. In: STUMM, W. (ed.) Aquatic surface chemistry, John Wiley & Sons, New York.

BRADBURY, M.H. & BAEYENS, B. (1994): Sorption by cation exchange: Incorporation of a cation exchange model into geochemical computer codes. PSI Bericht Nr.94-07, Paul Scherrer Institut, Villigen, Switserland and Nagra Technical Report NTB 94-11, Nagra, Wettingen, Switzerland.

BRUGGENWERT, M.G.M. & KAMPHORST, A. (1982): Survey of experimental information on cation exchange in soil systems.- In: BOLT, G.H. (ed.): Soil chemistry B. Physico-chemical models. Elsevier, Amsterdam.

CHARLET, L., SCHINDLER, P.W., SPADINI, L., FURRER, G. & ZYSSET, M. (1993): Cation adsorption on oxides and clays: The aluminium case. Aquatic Sci. 55, 291-303.

DAVIES, C.W. (1962): Ion association. Butterworths, London.

DAVIS, J.A. & KENT, D.B. (1990): Surface complexation modelling in aqueous geochemistry. In: HOCHELL, Jr., M.F. & WHITE, A.F. (eds.): Mineral-water interface geochemistry. Reviews in Mineralogy 23, 177-260.

DE LEVIE, R. (1990): Notes on Gouy diffuse-layer theory. J. Electroanal. Chem. 278, 17-24.

DZOMBAK, D.A., & MOREL, F.M.M. (1990): Surface complexation modelling. John Wiley & Sons, New York.

FLETCHER, P. & SPOSITO, G. (1989): The chemical modelling of clay/electrolyte interactions for montmorillonite. Clay Minerals 24, 375-391.

GAINES, G.I. & THOMAS, H.C. (1953): Adsorption studies on clay minerals. II. A formulation of the thermodynamics of exchange adsorption. J. Chem. Phys. 21, 714-718.

GREENLAND, D.J. & MOTT, C.J.B. (1978): Surfaces of soil particles. In: GREENLAND, D.J. & HAYES, M.B.H. (eds.): The chemistry of soil constituents. John Wiley & Sons, New York.

GRIM, R.E. (1953): Clay mineralogy. McGraw Hill, New York.

HUANG, C.P. & STUMM, W. (1973): Specific adsorption of cations on hydrous γ-Al_2O_3. J. Colloid Interface Sci. 43, 409-420.

HUNTER, R.J. (1981): Zeta potential in colloid science. Academic Press, London.

JAMES, R.O. & PARKS, G.A. (1982): Characterisation of aqueous colloids by their electrical double-layer and intrinsic surface chemical properties. In: MATIJEVIC, E. (ed.): Surface and colloid science 12, Plenum Press, New York, 119-216.

LAGALY, G. & FAHN, R. (1982): Ton und Tonminerale. In Ullmans Encyklopädie der technischen Chemie, 4 Aufl. 23. Verlag Chemie.

MAES, A., PEIGNEUR, P. & CREMERS, A. (1976): Thermodynamics of transition metal ion exchange in montmorillonite. Proc. Int. Clay Conf. 1975, 319-329.

NEWMAN, A.C.D. (1987): Chemistry of clays and clay minerals. Mineralogical Soc. Monograph No. 6, Longman.

PEARSON, JR., F.J., & BERNER, U. (1991): Nagra thermochemical data Base: I. Core data. Nagra Technical Report NTB 91-17. Nagra. Wettingen, Switzerland.

PEARSON, JR. F.J., BERNER, U. & HUMMEL, W. (1992): Nagra thermochemical data base II. Supplemental data 05/92. Nagra Technical Report NTB 91-18, Nagra, Wettingen, Switzerland.

SCHINDLER, P.W. & STUMM, W. (1987): The surface chemistry of oxides, hydroxides, and oxide minerals. In: STUMM, W. (ed.): Aquatic surface chemistry, John Wiley & Sons, New York

SPOSITO, G. (1984): The surface chemistry of soils. Oxford University Press, New York.

STUMM, W. & MORGAN, J.J. (1981): Aquatic chemistry (2nd ed.). John Wiley, New York.

STUMM, W., HUANG, C.P. & JENKINS, S.R. (1970): Specific chemical interactions affecting the stability of dispersed systems. Croat. Chem. Acta 42, 223-244.

VAN OLPHEN, H. (1963): An introduction to clay colloid chemistry. Interscience Publ., New York.

WAITE, T.D., DAVIS, J.A., PAYNE, T.E., WAYCHUNAS, G.A. & XU, N. (1994): Uranium (VI) adsorption to ferrihydrite: Application of a surface complexation model. Geochimica et Cosmochimica Acta 58, 5465-5478.

WANNER, H., ALBINSSON, Y., KARNLAND, O., WIELAND, E., WERSIN, P. & CHARLET, L. (1994): The acid/base chemistry of montmorillonite. Radiochimica Acta 66/67, 157-162.

WESTALL, J. (1982): FITEQL - A program for the determination of chemical equilibrium constants from experimental data. Version 2.0.- Technical Report, Chemistry department, Oregon State University, Corvallis, Oregon.

WESTALL, J., ZACHARY, J.L., & MOREL, F. (1976): MINEQL: A computer program for the calculation of chemical equilibrium composition of aqueous systems. Technical Note 18, Dept. of Civil Eng., Massachusetts Institute of Technology, Cambridge, Massachusetts.

YARIV, S. & CROSS, H. (1979): Geochemistry of colloid systems. Springer-Verlag, Berlin.